UCLouvain

École polytechnique de Louvain

Vitrimers as a solution to improve the viscoelastic and mechanical properties of recycled polymers

Author: **Alexandru Tudor BOBORODEA**
Supervisor: **Evelyne VAN RUYMBEKE**
Readers: **Bernard NYSTEN, Naïma SALLEM**
Academic year 2022–2023
Master [120] in Chemical and Materials Engineering

Contents

Acknowledgements

I would like to express my immense gratitude towards my supervisor, Professor Evelyne van Ruymbeke, for her guidance all throughout this work.

I am grateful to Professor Bernard Nysten for sharing his invaluable knowledge on AFM.

The challenges in sample preparation became surmountable with the precious help of Dr. Naïma Sallem and Pascal Van Velthem, and for this I am thankful.

The fruitful collaboration with the group of Professor Renaud Nicolay of ESPCI Paris allowed that the materials required in this project be available from the very beginning of this work. I am grateful to Ibrahim Göde for spending a week in our laboratory allowing me a deeper understanding of the synthesis and the preparation of vitrimer materials.

A common challenge during a thesis is that part of the instruments can fail. In this desperate situation, the possibility to perform the analyses at the other teams of UCLouvain became invaluable. I am very happy and grateful that this collaboration exists inside the university. Many thanks to Jean-François Statsyns for the DSC analyses and to Clément Coutouly for the GPC analyses.

The friendly ambiance inside the Rheology Group, with open discussions on very complex subjects, allowed me to better understand details on materials science. For all these discussions with all members of this group, I am very grateful. My thanks to Ophélie Ranwez who kindly provided some DSC results present in Figure 4.4.1.

For the unfailing support and the continuous encouragement throughout my entire life to reach my dreams, I express my very profound gratitude to my parents.

Abstract

Today, the mechanical recycling of polymers seems to be an essential step to address environmental issues related to plastics as it reduces the need to extract new raw materials and reduces the plastic waste generated. However, due to their poor physical properties, mechanically recycled plastic waste accounts for less than 10% of the feedstock used to manufacture new products in the European Union. To achieve the European Strategy goals of recycling 50% of plastic waste by 2030 requires developing new solutions to ensure that the mechanical and viscoelastic properties of the material are maintained at each life cycle.

A possible solution to address this challenge is to use dynamic covalent networks (e.g., vitrimers) which offer the combined advantages of thermoplastics and thermosets. Behaving as crosslinked polymers at low temperature, these materials stay, however, reprocessable at high temperature. Moreover, when added in low concentrations in polymer blends, they could also be used to reinforce the polymer-polymer interfaces, offering a promising way to improve the processing and mechanical properties of recycled polymers. As a first step towards the development of this method, the main objective of this work is to explore the dynamics of well-defined vitrimers in function of different parameters (such as their chemistry, molar mass, crosslinking density, or temperature), which will then be used as compatibilizers in immiscible blends.

This approach is investigated on two incompatible polymers: polystyrene (PS) and poly(2-ethyl hexyl methacrylate) (PEHMA), and on their blend. These polymers are specifically selected for their immiscibility translated by poor mechanical properties of their blends. Each thermoplastic as well as the PS based vitrimers and PEHMA based vitrimers are characterized by several analytical methods to understand their mechanical and rheological properties.

The Atomic Force Microscopy (AFM) results on the prepared blends without vitrimers show the incompatibility of the selected polymers. The Small Amplitude Oscillatory Shear (SAOS) experiments demonstrate a positive effect on the viscoelastic properties in the samples containing low concentrations of vitrimers.

Part 1 Introduction

Polymers are found everywhere in our daily lives and can be classified in many different ways. Before introducing the vitrimer, an interesting classification of polymeric samples is based on their response to heat and is related to the underlying molecular structure: the two main classes of polymers are thermoplastics and thermosets. As we will discuss later, vitrimers try to capture the advantages of both thermoplastics and thermosets.

Section 1.1 Thermoplastic and Thermoset Polymers

This section introduces the fundamental concepts of thermoplastic and thermoset polymers, along with their main properties. The objective is to emphasize the significant distinctions between the two, as well as the benefits and drawbacks of each, particularly in terms of recycling and mechanical properties.

1.1.1 Thermoplastic polymers

A thermoplastic is a type of polymer that can be reshaped or is mouldable when heated above the glass transition temperature T_g (or the melting temperature T_m for semicrystalline polymers). The polymer chains are not connected via chemical bonds but can be entangled if the molar masses are significantly large. At low temperature, below T_g, they behave as solid materials. The key advantage of a thermoplastic is its recyclability as it can be melted and reshaped multiple times without undergoing any significant chemical changes. Thermoplastics are used in a wide range of applications due to their versatility and ease of processing. They are commonly found in the manufacture of consumer goods such as toys, containers, and packaging materials [1].

In addition to their recyclability and versatility, thermoplastics have other advantages such as their energy efficiency in manufacturing and processing. Thermoplastic components can be made in very high volumes with high precision and low cost. For instance, high-density poly(ethylene) (HDPE) has a market value that ranges from 0.96 to 0.98 Euro per kilogram [2]. In some cases, thermoplastic polymers can even replace metals with considerable weight

savings if proper care is taken in the design. Most thermoplastics can tolerate larger deflections than metals without deforming [3].

Generally, an important drawback of thermoplastics is their poor mechanical properties at high temperatures rendering them unsuitable for high-temperature applications where they could deform and/or flow.

1.1.2 Thermoset polymers

The main drawback of thermoplastics is overcome by thermosets. A thermoset is a type of polymer material that is able to withstand high temperatures without deformation or chemical changes. This property is made possible by the presence of crosslinking between the polymer chains, which are irreversible chemical bonds, making the material more durable than thermoplastic materials. However, this durability has a major drawback as it renders the material difficult to recycle. Indeed, once synthesized, a thermoset cannot be reshaped or remoulded [4].

Due to their extraordinary stability, thermosets have widespread use in a variety of applications. They are commonly used as adhesives, coatings, insulation, and mould compounds. They are also used for manufacturing permanent parts in a wide array of industries such as electrical goods and construction equipment panels and insulators [4]. A thermoset can be used either below its glass transition temperature as a solid material, or above the glass transition temperature as an elastomer (e.g., rubber).

In terms of cost, the current market value of one kilogram of polyester resin is in the range of 1.65 Euro to 1.74 Euro [2]. For epoxy resins, the market value ranges from 3.46 Euro to 5.11 Euro per kilogram [2]. It is important to mention that, for some thermosets, the price can reach up to 50.00 Euro per kilogram. Factors that can affect the cost of thermosets include the specific polymer chemistry, market demand, and regional factors such as taxes and environmental regulations.

Section 1.2 Vitrimers

Both thermoplastics and thermosets have their own unique advantages and disadvantages. However, material scientists have been striving to develop a new material that combines the benefits of both while avoiding their respective drawbacks. This section introduces the concept of a vitrimer and provides a comprehensive discussion on its thermal, chemical, and mechanical properties. Additionally, a detailed definition of this innovative material is provided.

In 2005, French chemist J.-M. Lehn introduced the term "dynamers" [5] to describe polymer systems that can change their molecular structure through dynamic bond exchange. These systems can be either molecular or supramolecular, depending on whether the connections between the chains are reversible covalent bonds or non-covalent interactions. Molecular dynamers use reversible covalent bonds to connect the chains, while supramolecular dynamers use non-covalent interactions such as metal-ligand or hydrogen bonding.

In 2010, C. N. Bowman and his colleagues proposed a more precise concept called a "covalent adaptable network" (CAN) [6] to describe dynamic polymer systems that use dynamic covalent bonds. A dynamic covalent bond is a type of covalent bond that can quickly reach thermodynamic equilibrium when exposed to a stimulus such as heat or light. This allows the bond to break and reform rapidly, enabling the polymer system to change its topology.

The bond exchange in a covalent adaptable network can occur through either a dissociative or associative mechanism. In a dissociative dynamic bond exchange, the crosslinks undergo two separate steps of breaking and reforming. An example of such a reaction is the Diels-Alder exchange process. In an associative mechanism, the breaking and reforming occur simultaneously, allowing for constant crosslinking (i.e., constant connectivity of the network) throughout the process. Several examples have already been demonstrated using transesterification and dioxaborolane metathesis reactions [7] [8].

In 2011, L. Leibler and his co-workers introduced the term "vitrimer" to refer to a covalent adaptable network that uses an associative mechanism for bond exchange [7]. A vitrimer has two characteristic temperatures: a glass transition temperature (T_g) and a freezing topology temperature (T_v), which is defined as the temperature at which the melt viscosity is equal to 10^{12} Pa · s [9]. At a temperature higher than T_v ($T_g < T_v < T$), the exchange reactions are fast compared to the motion of the polymer chains and the material is able to flow. At a temperature T such as $T_g < T < T_v$, the material behaves like an elastomer, meaning it can stretch and deform but will return to its original shape when the stress is removed. At a low temperature ($T < T_g < T_v$), the material is glassy and behaves like a solid. The word "vitrimer" comes from the silica-like behaviour of these materials because the change in viscosity with temperature is much milder than for thermoplastics, making processing easier [10].

Vitrimers have many potential applications due to their unique combination of properties. They combine the strength and stability of thermosets with the processability of thermoplastics. This makes them ideal for use in applications requiring strength and adaptability. In addition to their mechanical properties, vitrimers also have unique chemical properties allowing them to change their chemical structure in response to changing conditions. One potential application of this property is in the field of self-healing materials to create materials that can repair themselves when damaged by reforming the broken bonds [10]. This allows materials such as coatings or structural components to last longer and require less maintenance. Most importantly, the unique properties of vitrimers make them recyclable. A major inconvenience however is their high production cost limiting their use on an industrial scale.

Overall, vitrimers can be defined as a class of plastics derived from thermosetting polymers that consist of molecular covalent networks able to change their topology via thermally activated bond-exchange reactions. They are a subset of covalent adaptable networks, which are a class of polymer material capable of self-healing and shape reprocessing at temperatures above their topology freezing temperature T_v where dynamic covalent bond exchange reactions dominate.

Section 1.3 Recycling

The recycling of polymers is a complex issue that requires an extensive understanding of the materials involved as well as the processing techniques currently used in recycling. This section aims at highlighting the difficulties and the challenges that are being faced in this field, and to explore the potential solution of using vitrimers as a strategy to overcome these obstacles.

Annually, the global plastic production reaches an astonishing 450 million metric tons [11] [12], with the European Union alone producing nearly 65 million metric tons in 2022 [13]. Plastic production is utilized in various sectors, with packaging accounting for 40%, building and construction for 20%, and automotive for 10%. The household sector contributes for 4% to the overall usage [14]. As a result, plastic objects have become present in every aspect of our daily lives. However, despite this widespread use, our ability to recycle end-of-life plastic products remains quite limited.

In the European Union, approximately half of the plastic waste collected is exported to other countries (outside the European Union) for treatment because of "a lack of capacity, technology, and financial resources" [14]. An important part of the remaining stock is landfilled or used for energy recovery, which releases large amounts of greenhouse gases, detrimental to the environment. Only about 10% of the feedstock is actually mechanically recycled [15].

However, recent developments have led to an increasing demand for local treatment of plastic waste. China has enforced restrictions on plastic waste imports in 2018. The European Strategy for Plastics in a Circular Economy proposed in 2018 that "by 2030, more than half of plastics waste generated in Europe is recycled" [16]. The Green Deal, proposed by the European Commission, has been approved by the European Council in 2021 [17]. These events have emphasized the need for an efficient and local treatment. A promising strategy is to increase the fraction of plastics that are mechanically recycled.

To achieve this goal however, there are several difficulties that must be addressed. Major issues include the quality and price of recycled products compared to "virgin" products. The low fraction of mechanically recycled plastics is particularly due to the poor mechanical and chemical properties of the end-products manufactured. Additionally, processing and manufacturing require large feedstocks with strictly known specifications and compositions which may vary depending on the source or the provider.

One of the main challenges in the recycling process is the sorting step as the final polymer may contain 5% to 10% impurities that are often incompatible with the major phase. These impurities tend to phase separate into nodules, leading to reduced mechanical or chemical properties, and thermal stability. This is due to weak properties at the interface. As a result, these interfaces are unable to withstand large stresses, which can be problematic for some industrial applications. To address this limitation, it is proposed to incorporate vitrimers to reinforce the properties at the interface by creating covalent dynamic bonds between the two phases. This concept is illustrated in Figure 1.3.1.

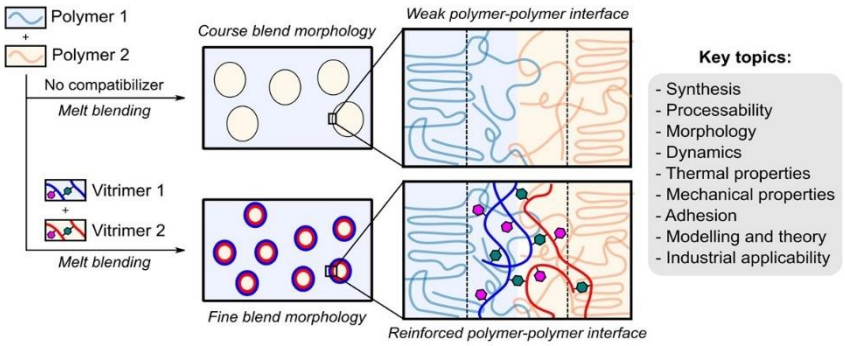

Figure 1.3.1: Illustration of the concept of adding vitrimers as compatibilizer with the aim to reinforce the interface between the two incompatible polymers. Picture provided by Nathan Van Zee (ESPCI, Paris), in the framework of the EU doctoral network "ReBond".

This approach can significantly enhance the mechanical and chemical properties of the entire material, paving the way for a more efficient recycling process of polymers. The ultimate goal is to achieve high mechanical properties, similar to thermosets, while also enabling the recycling of this type of material.

Section 1.4 Project Objectives

This section provides the main objective of this research project. A detailed description of the specific objectives of this master thesis is also provided.

The main objective of this research project is to investigate the possibility of using vitrimers as universal compatibilizers allowing to increase the recycled fraction of contaminated plastic waste.

To attain this goal, a crucial point is a deep understanding of the modification of mechanical and rheological properties of immiscible polymer blends in the presence of vitrimers. Therefore, the first objective of this master thesis is to select and characterize the raw materials to obtain a well-defined immiscible polymer blend simulating a contaminated plastic waste. Furthermore, the mechanical and rheological properties of homopolymers, as well as their respective vitrimer materials are investigated, the goal being to understand the fundamental differences in mechanical and rheological properties between the two types of materials, and the influence of several parameters such as their nature, molar mass, crosslinking density, as well as the temperature of measurement.

Part 2 Fundamentals

In order to comprehend the behaviour of polymer materials and address the current challenges associated with plastic recycling, rheology is an invaluable tool that can be used to establish a link between the viscoelastic properties and the chemistry of the materials investigated. Additionally, molecular models can be implemented and integrated to establish a correlation between the macroscopic and microscopic data and provide a comprehensive understanding of the material behaviour. Important concepts of atomic force microscopy are also presented in this part as this characterization technique is an effective tool in highlighting phase separation in a polymer blend sample.

Section 2.1 Fundamentals in Linear Viscoelasticity

This section describes important concepts and ideas related to the field of rheology. The relaxation modulus of a polymer material is defined, and an explanation is provided on the oscillatory shear experiment to measure the storage and loss moduli. The aim is to understand the fundamental parameters governing the behaviour of a polymer material under different experimental and/or processing conditions.

2.1.1 Rheology

Rheology is the study of the deformation and flow of matter and describes the interconnection between these concepts with time and temperature. Rheological properties are useful to evaluate the performance of a material during processing operations. Industrial processes such as extrusion and injection moulding require understanding flow properties to optimize the parameters available. In materials engineering, the mechanical properties of a polymer are closely related to changes in the microstructure. A rheological study on materials provides an insight to uncovering and identifying these changes [18].

2.1.2 Stress Relaxation and Relaxation Modulus

The behaviour of a viscoelastic material undergoing a stress σ or a deformation γ is a combination of an elastic response and a viscous response, which is dependent on the time frame of the observation. An important rheological experiment for a viscoelastic material is a step shear strain experiment. In this experiment, a shear strain of amplitude γ_0 is applied to a sample at time t_0. The shear stress is measured as a function of time t. The relaxation modulus $G(t, \gamma)$ is defined as the ratio between the measured stress and the applied strain. It is important to note that many experiments are performed in the "linear regime" where the relaxation modulus is independent of the strain applied (i.e., small deformation). In practice however, the relaxation modulus cannot be accurately established over the entire range of time. Some difficulties arise from instrument limitations and long-time sample stability. The precision of the experimental data is also limited by the complexity of generating an instantaneous strain. Measuring the rapid decay of the stress at short times and the small stress at long times presents another challenge [18].

2.1.3 Oscillatory Shear Experiment

The oscillatory shear experiment avoids the issues cited and accurately determines the relaxation modulus of a material. In a controlled strain oscillatory shear experiment, a sinusoidal shear strain is applied to a sample.

$$\gamma(t) = \gamma_0 \cdot \sin(\omega \cdot t) \tag{2.1.1}$$

If the experiment is performed in the linear regime (i.e., small deformation), the response is also a sinusoidal function and can be written in terms of the stress amplitude σ_0 and loss angle δ. The method is called Small Amplitude Oscillatory Shear (SAOS).

$$\sigma(t) = \sigma_0 \cdot \sin(\omega \cdot t + \delta) \tag{2.1.2}$$

2.1.4 Storage and Loss Moduli

Using trigonometric identities, it is possible to develop the stress as follows:

$$\sigma(t) = \sigma_0 \cdot [\, \sin(\omega \cdot t) \cdot \cos(\delta) + \cos(\omega \cdot t) \cdot \sin(\delta) \,] \tag{2.1.3}$$

A relaxation modulus G_d may be defined as the ratio between the amplitude stress σ_0 and the amplitude strain γ_0 allowing further development in the above expression:

$$\sigma(t) = \gamma_0 \cdot [\, G_d \cdot \sin(\omega \cdot t) \cdot \cos(\delta) + G_d \cdot \cos(\omega \cdot t) \cdot \sin(\delta) \,] \tag{2.1.4}$$

Experimental data from Amplitude Oscillatory Shear is often reported using the storage and loss moduli as functions of frequency i.e., $G'(\omega)$ and $G''(\omega)$. These material functions can be highlighted as follows:

$$\sigma(t) = \gamma_0 \cdot [\, G'(\omega) \cdot \sin(\omega \cdot t) + G''(\omega) \cdot \cos(\omega \cdot t) \,] \tag{2.1.5}$$

It is sometimes interesting to consider that the storage and loss moduli are respectively the real and imaginary components of the complex modulus, denoted $G^*(\omega)$ and defined as:

$$G^*(\omega) = G'(\omega) + i \cdot G''(\omega) \tag{2.1.6}$$

In this interpretation, the parameter G_d is the magnitude of the complex modulus, and the loss angle δ is the angle formed by the storage and loss moduli in the complex plane. Knowing the storage and loss moduli with high precision and over a sufficiently large range of frequencies allows for complete characterisation of the viscoelastic behaviour of the studied material in the linear regime. For the implementation of a rheological model, it is useful to link the storage and loss moduli to the relaxation modulus.

One can show that:

$$G'(\omega) = \omega \cdot \int_0^{\infty} G(s) \cdot \sin(\omega \cdot s) \cdot \mathrm{d}s \tag{2.1.7}$$

$$G'(\omega) = \omega \cdot \int_0^{\infty} G(s) \cdot \cos(\omega \cdot s) \cdot \mathrm{d}s \tag{2.1.8}$$

In principle, these expressions can be inverted to obtain the relaxation modulus, but it is more common to use numerical methods, such as proposed by F. R. Schwarzl, to switch between the frequency domain and the time domain (and vice versa) [19-21].

2.1.5 Loss or Phase Angle

As mentioned earlier, the loss angle, also referred to as the phase angle, is the angle formed by the storage and loss moduli in the complex plane. The angle is denoted by δ and can be computed using:

$$\tan(\delta) = \frac{G''}{G'} \tag{2.1.9}$$

Section 2.2 Time Temperature Superposition Principle

This section describes the Time Temperature Superposition principle and introduces the shift factors. The temperature dependencies with the Arrhenius and Williams-Landel-Ferry models are presented. A brief discussion on the validity of this principle is also provided.

2.2.1 Working Principle

In a standard oscillatory shear experiment, one should note that the data collected is effective over a limited range of frequencies, due to instrument limitations. This range is usually between 10^{-1} rad/s and 10^{2} rad/s. It is however possible to extend the set of data points by performing the experiment at different temperatures over this limited range. The data is then shifted according to a reference temperature T_{ref} to create a plot with an extended frequency range [18].

2.2.2 Time or Frequency Shift Factors

The time or frequency shift corresponds to a horizontal shift of an experimental data set. It is characterized by a shift factor noted a_T. This concept allows one to define a reduced frequency ω_r as:

$$\omega_r = \omega \cdot a_T \tag{2.2.1}$$

To describe the temperature dependence of the horizontal shift factors, several empirical expressions have been proposed. The most common ones are the Arrhenius dependence and the Williams-Landel-Ferry (WLF) dependence. These expressions use parameters such as the activation energy for flow E_a and empirical constants C_1 and C_2 that are dependent on the chosen reference temperature.

$$a_T(T) = \exp\left[\frac{E_a}{R} \cdot \left(\frac{1}{T} - \frac{1}{T_{ref}}\right)\right] \quad \text{(Arrhenius)} \tag{2.2.2}$$

$$\log\left(a_T(T)\right) = \frac{-C_1 \cdot \left(T - T_{ref}\right)}{C_2 + T - T_{ref}} \quad \text{(Williams-Landel-Ferry)} \tag{2.2.3}$$

2.2.3 Modulus Shift Factors

The modulus shift corresponds to a vertical shift of an experimental data set and accounts for the effect of temperature on the density of the material ρ. The vertical shift factor is noted b_T and is defined as:

$$b_T = \frac{T_{ref} \cdot \rho_0}{T \cdot \rho} \tag{2.2.4}$$

As in the case of the horizontal shift, a reduced modulus G_r may be defined as:

$$G_r = G(T) \cdot b_T \tag{2.2.5}$$

When shifting experimental data sets, it is common to use $\tan(\delta)$ instead of the storage and loss moduli. This is because in $\tan(\delta)$ the vertical shift factors are cancelled out.

2.2.4 Validity of the Time Temperature Superposition

The Time Temperature Superposition (TTS) principle is valid if "the characteristic times for all the relaxation mechanisms involved over the range of reduced frequencies or times of concern have the same temperature dependence" [18]. In other words, all the relaxation phenomena occurring in the material have the same temperature dependence. In this case, the material is thermo-rheologically simple. Some materials, such as long-chain branched polymers, reversible polymer networks and chemically heterogenous samples (i.e., polymer blends), may not exhibit time temperature superposability. An overlap of relaxation mechanisms can be present, and a thermo-rheological complexity is observed. Examples where the Time Temperature Superposition principle fails are reviewed by D. J. Plazek [22] who also highlighted the possibility to identify and separate relaxation mechanisms.

Section 2.3 Molecular Rheological Models

This section explains several models used to describe the rheological properties of polymer materials. The implementation of simulations and models on experimental data is effective in highlighting information on the underlying characteristics of the material, such as its molar mass distribution and its molecular structure. It also provides information on the processing characteristics of the material. In particular, the Time Marching Algorithm, developed at Université catholique de Louvain, is used later in this thesis to analyse the experimental results related to this project.

2.3.1 Coarse-Grained Model

The dynamics of a single polymer molecule is difficult to model with an atomically detailed representation, as a large amount of information (e.g., number of chemical bonds, motion limitations, atomic interactions) must be considered. Computational tasks remain complex even with current resources. As such, coarse grained models are useful to simplify the description of the molecule without compromising important physical properties. An approach is to consider the polymer as a freely jointed Gaussian chain consisting of an ensemble of sub-chains. One may picture the sub-chains as Kuhn segments. Each Kuhn segment includes a significant number of monomer units, such that the orientations of two consecutive segments are not correlated. Consequently, the chain can be seen as a random walk made of Kuhn steps. It follows that this coarse-grained representation is only appropriate for polymers with sufficient high molar masses [18]. In this work, the total number of Kuhn segments present in a single polymer molecule is noted n. The length of one Kuhn segment is noted b.

2.3.2 Dumbbell Model

The physical characteristics of a polymer molecule are governed by its entropic elasticity (determined by thermal motion). To account for this property, one can visualize the polymer chain as a dumbbell element: a spring connecting two beads. In this representation, it is possible to derive an expression for the entropy of the polymer chain. A relaxation time can then be determined, which is denoted by τ_R.

2.3.3 Linear Polymer in a Dilute Solution

The model proposed by P. E. Rouse in 1953 [23] provides a comprehensive understanding of the behaviour of a polymer molecule in a dilute solution, where the polymer molecules are regarded as non-interacting molecules. The model uses a coarse-grained representation as it also considers a polymer molecule as a set of n sub-chains, or Kuhn segments, each represented by a dumbbell element. The mass of a Kuhn segment is assumed to be concentrated in a single bead, located at its centre. The beads are connected to each other by springs.

At very short time scales (at $t \approx 0$), the conformation of the polymer chain is almost identical to the initial conformation (at $t = 0$). In this case, each Kuhn segment contributes with an energy amount of $k_B \cdot T$ to the stress required to keep the polymer chain deformed [24]. At this time, the corresponding modulus can be computed as:

$$G(t \approx 0) = \nu \cdot k_B \cdot T \cdot n \tag{2.3.1}$$

with ν the number density of polymer chains in the solution.

As the time scale of the observation increases, the polymer chain progressively loses the correlation between its current and initial orientations. The phenomenon initially occurs at very short (or local) length scales, and afterwards at larger length scales. These length scales are defined as "modes" of relaxation. In this framework, the mode p refers to a chain segment of molar mass M/p where M denotes the molar mass of the polymer molecule [24]. The time required to relax this segment is noted τ_p. The modulus corresponding to the mode p is computed as follows:

$$G\left(t = \tau_p\right) = \nu \cdot k_B \cdot T \cdot p \tag{2.3.2}$$

The relaxation time corresponding to the mode p is given by:

$$\tau_p = \frac{\zeta_0 \cdot b^2 \cdot n^2}{3 \cdot \pi^2 \cdot k_B \cdot T \cdot p^2} \approx \tau_0 \cdot \left(\frac{n}{p}\right)^2 \tag{2.3.3}$$

with ζ_0 the friction coefficient of one Kuhn segment.

In a similar way, the relaxation modulus can be approximated by:

$$G(t) \approx \nu \cdot k_B \cdot T \cdot \sum_{p=1}^{n} \exp\left(-\frac{2 \cdot t}{\tau_p}\right) = \frac{\rho \cdot R \cdot T}{M} \cdot \sum_{p=1}^{n} \exp\left(-\frac{2 \cdot t}{\tau_p}\right) \tag{2.3.4}$$

2.3.4 Entangled Linear Polymer

Polymers are often processed as a concentrated solution or as a melt. The molar masses involved in these processes are also quite large (from 100,000 g/mol to 10,000,000 g/mol). The flexible polymer molecules are inevitably entangled. Therefore, the thermal motion of a polymer molecule is significantly restricted due to the presence of the surrounding molecules. The impediments to motion are referred to as "entanglements." In this framework, several models and relaxation processes must be introduced to accurately describe the relaxation of an entangled polymer molecule.

Rouse Relaxation Process

The fast relaxation modes (FR) can take place in this case as they involve a local motion of the chain segments. At short observation time scales, the influence of the neighbouring polymer molecules can therefore be overlooked. As the time scale increases however, the polymer molecule progressively "feels" the other molecules present. In a way, at short time, the entanglements act as physical cross-linking points, preventing the further relaxation of higher modes [24]. The longest chain segment, which is able to relax via this Rouse process, is referred to as "entanglement segment." Its molar mass is denoted by M_e and the corresponding relaxation time is denoted by τ_e. It follows that a polymer molecule is composed of $Z = M/M_e$ entanglement segments.

At the time τ_e, the relaxation modulus is equal to:

$$G(t = \tau_e) = \nu \cdot k_B \cdot T \cdot Z = \frac{\rho \cdot R \cdot T}{M} \cdot Z = \frac{\rho \cdot R \cdot T}{M_e} \tag{2.3.5}$$

This value is referred to as "entanglement modulus" and is denoted G_e. The modulus cannot further decrease due to the constraints on the polymer molecule. In practice however, it is observed that around one fifth of this value is lost due to a partial Rouse relaxation process occurring for higher modes. These segments can move along the backbone of the polymer molecule. Such phenomena are referred to as longitudinal Rouse modes (LR). After the fast Rouse modes and the longitudinal Rouse modes, the polymer molecule reaches an equilibrium state. The modulus corresponding to this state is called the "plateau modulus" (or "rubbery plateau") and is equal to:

$$G_N^0 = \frac{4}{5} \cdot \frac{\rho \cdot R \cdot T}{M} \cdot Z = \frac{4}{5} \cdot \frac{\rho \cdot R \cdot T}{M_e} \tag{2.3.6}$$

Tube Model

In the rubbery plateau regime, the polymer molecules cannot further relax via a Rouse process. Three material parameters can be defined as in the tube theory model: the plateau modulus G_N^0 the molar mass of an entanglement segment M_e and the relaxation time of an entanglement segment τ_e. It is important to keep in mind that the parameters G_N^0 and M_e are linked by equation $(2.3.6)$. These parameters are independent on the architecture or the molar mass of the polymer.

At this stage of the relaxation process, it is useful to consider a new coarse-grained representation of the polymer molecule with the entanglement segment as the smallest unit, as an alternative to the Kuhn segment. The polymer molecule can be considered trapped in a tube. This model was first proposed by P.-G. de Gennes [25] and later extended by M. Doi and S. F. Edwards [26]. One can compute the most probable curvilinear path length of the polymer chain, denoted L_{eq}, as equal to $Z \cdot l$ where l is the length of an entanglement segment.

Assuming an entanglement segment also behaves as a Gaussian chain moving along the tube, these values are related to each other as follows:

$$R^2 = n \cdot b^2 = Z \cdot n_e \cdot b^2 = Z \cdot l^2 = L_{eq} \cdot l \tag{2.3.7}$$

where R^2 represents the quadratic end-to-end distance of the polymer chain.

To further describe the relaxation of the polymer molecule, it is necessary to introduce other relaxation mechanisms. There are three important processes that have been discovered by which linear polymer molecules can escape from the tube and relax: reptation, contour length fluctuations and constraint release. These three mechanisms are illustrated in Figure 2.3.1.

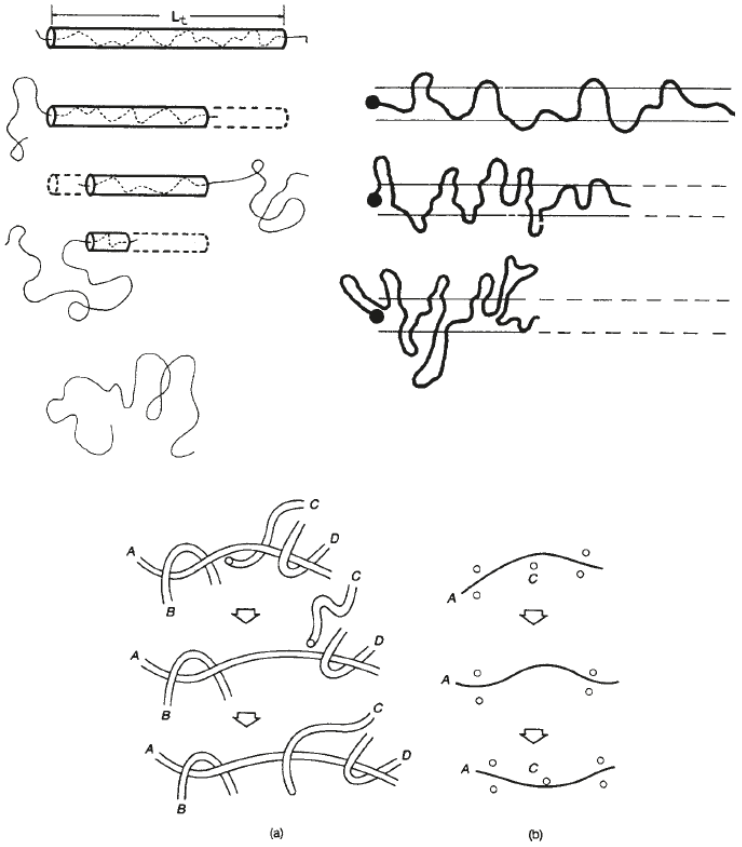

Figure 2.3.1: Illustration of three relaxation mechanisms: (Upper left) Reptation of a polymer molecule out of its tube. The tube is straightened to aid visualization. (Upper right) Contour Length Fluctuations of a polymer molecule. The motion of the chain end allows the molecule to explore new regions. (Bottom) Constrain Release in which the motion of chain "C" releases a constraint for chain "A" allowing it to relax [18].

Reptation

Reptation refers to a thermally activated motion of the polymer molecule along the curvilinear axis of the tube. This relaxation process can be described by a one-dimensional diffusion equation. The polymer chain can slowly escape the tube by moving back and forth along the axis, and progressively lose the correlation between the current and initial conformations. The curvilinear diffusion coefficient is denoted D. It is dependent on the friction (or drag) force applied on each Kuhn segment, or equivalently it is dependent on the friction factor of a Kuhn segment ζ_0. The diffusion coefficient can be computed as follows:

$$D = \frac{k_B \cdot T}{n \cdot \zeta_0} \tag{2.3.8}$$

The time needed to relax the polymer chain via a reptation process is given by:

$$\tau_{rept} = \frac{L_{\text{eq}}^2}{\pi^2 \cdot D} = \frac{\zeta_0 \cdot n_e^2 \cdot b^2}{\pi^2 \cdot k_B \cdot T} \cdot \left(\frac{M}{M_e}\right)^3 = 3 \cdot \tau_e \cdot Z^3 \tag{2.3.8}$$

Contour Length Fluctuations

To accurately model the relaxation of an entangled linear polymer molecule, it is necessary to consider that the outer segments of the chain have more degrees of freedom than the inner segments. The outer segments are not constrained by the tube, implying that the corresponding relaxation time is shorter. In this framework, the position of a segment is introduced and noted by x. A position $x = 0$ refers to the chain extremity, and a position $x = 1$ refers to the middle of the chain [24]. An estimation for the required time to relax a segment at a position x along the curvilinear path of the tube is given by:

$$\tau_{early} = \frac{9 \cdot \pi^3}{16} \cdot \left(\frac{M}{2 \cdot M_e}\right)^2 \cdot \tau_R \cdot x^4 \tag{2.3.8}$$

Constraint Release

In addition to the reptation and contour length fluctuations mechanisms, another process must be taken into account. This relaxation process considers the surrounding polymer molecules are also able to move and to relax. Therefore, an entanglement can also be lost if another chain releases it by diffusion. This means that the constraints applied on the polymer test molecule are reduced, which in turn implies that the tube is dynamic and its diameter should increase with time. This is called Dynamic Tube Dilation (DTD) theory. Only the fraction effectively constraining the test chain should be involved in the tube representation. The complete mathematical derivation is more complex than for the previous mechanisms and is not presented in this work.

2.3.5 Time Marching Algorithm

The Time Marching Algorithm (TMA) is a general coarse-grained model capable of predicting the linear viscoelastic properties of linear (and branched) polymers, provided that the molecular structure is known, and three viscoelastic parameters are provided: the relaxation time of an entanglement segment (τ_e), the plateau modulus (G_N^0), and the molar mass of the entanglement segment (M_e). The model is based on the tube theory and accounts for reptation, contour length fluctuations, constraint release and dynamic tube dilation.

This approach is based on an iterative computational algorithm of the relaxation of a set of polymer molecules. All the relaxation mechanisms are implemented as a function of time, which enables the determination of the relaxation modulus $G(t)$ of the polymer material at each observation time scale.

It is also important to consider the polydispersity of the polymer. The relaxation mechanisms of reptation and contour length fluctuations occur simultaneously for each polymer molecule but have a different influence depending on the molar mass. To address this issue, the algorithm computes both relaxation mechanisms in parallel. This is achieved by defining a survival probability function, denoted $y(t)$, which represents the fraction of the initial tube that still exists at time t. This approach can determine the unrelaxed fraction of polymer molecules present in the material. To calculate the relaxation modulus, the algorithm iterates over each relevant molar mass, and time.

Overall, this algorithm is a considerable advancement in the field of material sciences. The algorithm has been shown to provide excellent predictions for the linear viscoelastic properties of linear and complex macromolecular polymer architectures [27].

Section 2.4 Interfacial Slip Effect on the Rheological Behaviour of a Polymer Blend

This section highlights an experimental study performed by M. Bousmina et al. to understand the slip effect on the rheological behaviour of several poly(styrene) (PS) and poly(methyl methacrylate) (PMMA) blends. This study is particularly important as it can help understanding the phenomena occurring at the interface of two incompatible polymers.

2.4.1 Framework

As previously mentioned, one of the primary challenges in polymer recycling is the loss of mechanical properties due to the presence of an incompatible polymer within the main matrix. This presence results in a weak interface between the phases, leading to reduced mechanical strength and chemical resistance. In a study conducted by M. Bousmina et al. [28], various poly(styrene) (PS) and poly(methyl methacrylate) (PMMA) blends were analysed from a rheological standpoint, over a wide range of blend concentrations.

Dynamic experiments were conducted in the linear regime with a strain of 0.1. This value was confirmed by previous strain sweep measurements. Additionally, Scanning Electron Microscopy (SEM) analyses were conducted on each prepared blend to study the interface between the two phases.

2.4.2 Blend classification

When two polymers that are immiscible and have different viscosities are combined, the resulting mixture generally exhibits an intermediate viscosity in the high frequency range, between 10^0 rad/s and 10^2 rad/s. However, in the low frequency range, below 10^{-1} rad/s, the viscosity of the mixture is generally higher than that of the major phase. It is important to note that this is not always the case. For instance, L. A. Utracki [29] classified polymer blends into three categories based on their viscosity-concentration dependence in relation to the log-additivity rule $\log(\eta) = \sum_i \phi_i \cdot \log(\eta_i)$ where ϕ_i and η_i denote the volume fraction and viscosity of component i.

The three categories are as follows:

- PDB: blends showing a positive deviation from the log-additivity rule.
- NDB: blends showing a negative deviation from the log-additivity rule.
- PNDB/NPDB: blends showing both positive and negative deviations from the log-additivity rule.

The study found that the viscosity of blends with PS as the major phase is lower than the viscosity of both pure PS and PMMA. This indicates that PS – PMMA blends, with PS as the major phase, are NDBs. The negative deviation is attributed to "poor adhesion between the segregated domains of the blends, causing interfacial slippage during shear flow" [28]. The poor adhesion is believed to be due to a loss of entanglement between the polymer molecules of each phase.

In order to determine the relationship between a poor interfacial adhesion and the lack of entanglement between the polymer molecules at the interface, several PS – PMMA blends were prepared with a compatibilizer: poly(styrene)-*block*-poly(methyl methacrylate) (PS-*b*-PMMA) copolymer. A small amount of compatibilizer was incorporated during the mixing process, 1 wt.% with respect to the dispersed phase.

Interestingly, the addition of the interface modifier can suppress the interfacial slippage effect between the two phases. The study concludes that the interfacial slip originates from the loss of entanglements within the interface between the blend phases.

2.4.3 Interest within the scope of this study

The weakened interface between the blend phases results in poor mechanical and chemical properties. However, by creating covalent bonds between the polymer chains at the interface, it should be possible to reinforce these properties. This master thesis investigates this possibility based on the use of vitrimers. Additionally, the work of M. Bousmina [28] highlights the crucial role of rheology in the study of blends of incompatible polymers, by explaining the effect of a compatibilizer (even in small amounts) on the curves of the storage and loss moduli of the blend.

Section 2.5 Fundamentals in Atomic Force Microscopy

Atomic Force Microscopy (AFM) is a highly effective tool for analysing and characterizing material surfaces. It allows to distinguish between various phases and to study polymer compatibility by accessing the interface. The objective of this section is to describe the fundamental concepts of atomic force microscopy, including the key mathematical principles.

2.5.1 Working Principle

Atomic Force Microscopy (AFM) is an advanced characterization technique that enables the analysis of surface samples at the nanoscale level. The principle behind this technique involves measuring the interactive forces between a specialized probe, made of an elastic cantilever with a sharp tip at the end, and the surface sample. As the tip interacts with the surface, the cantilever bends, and the deflection of the cantilever is measured to evaluate the tip/surface interactive force. This process allows for extracting detailed information on the surface properties, such as topography, stiffness, and adhesion. There are various "modes" available, however, for this study, the peak-force tapping mode, which is a semi-contact mode, has been employed.

To understand the working principle of this mode, it is important to introduce the notions of forced oscillations of the cantilever and explain the non-contact mode. While this master thesis does not provide all the mathematical descriptions and derivations of these modes, interested readers can refer to the book Fundamentals in Scanning Probe Microscopy, by V. Mironov [30]. This book is very interesting for those seeking a deeper understanding of the subject.

2.5.2 Forced Oscillations of the Cantilever

In several modes of atomic force microscopy analyses, the cantilever of the probe is forced to vibrate at a specific frequency, denoted ω. The amplitude of the oscillations can be determined based on the equation of motion.

2.5.3 Non-Contact Mode

In the non-contact mode, the cantilever is forced to vibrate with a small amplitude of the order of 1 nanometre. As the probe approaches the surface of the sample, the cantilever encounters an extra-force, which arises from long-range attraction interactions, such as van der Waals forces. When this additional force is considered into the equation of motion, one notices another change in the frequency and amplitude of the oscillations.

2.5.4 Semi-Contact Mode

In the semi-contact mode (i.e., the one used in this master thesis), the cantilever is forced to oscillate near its resonance frequency with an amplitude ranging from 10 to 100 nanometres. The tip is brought closer to the surface until it can make a direct contact with the sample. In this case, the equation that describes the motion of the cantilever becomes non-linear. The characteristic features of semi-contact mode are similar to those of the previous modes. The amplitude and frequency of the oscillations are influenced by the interaction between the tip and the surface, with the unique aspect being the mechanical interaction between the two. In this case, the local stiffness of the sample also plays a role in the observed changes. It is important to note the capacity of this characterization technique to distinguish between different materials and/or phases based on changes in the tip/sample interactions, resulting from various forces present in the system. While material properties can be extracted from the analyses, this is beyond the scope of the present work.

Part 3 Materials and Methods

To understand the behaviour of polymeric materials and establish rheological models of vitrimers, it is imperative to obtain accurate and reliable experimental data. This part provides a comprehensive overview of the materials, procedures, and equipment utilized in this study. Additionally, it encompasses the type of data collected on the materials and samples investigated.

Section 3.1 Materials and Specifications

Poly(styrene) (PS) and poly(2-ethyl hexyl methacrylate) (PEHMA) are the main materials investigated in this work. These polymers have been chosen for their incompatibility. For the relevant samples, the synthesis methods are described, and the resulting properties are presented.

To attain the objectives outlined in Section 1.4, a list of specifications and requirements is developed for the two polymers that make up the system under investigation.

These two polymers are chosen to meet specific criteria:

- They must be incompatible.
- They must be sufficiently different, such as having different glass transition temperatures.
- There should be an easy-to-use method to determine the composition of the polymer blend.
- They must be amorphous.

Based on the given specifications and requirements, the chosen polymers are poly(styrene) (PS) and poly(2-ethyl hexyl methacrylate) (PEHMA). The chemical structure of each polymer is illustrated in Figure 3.1.1.

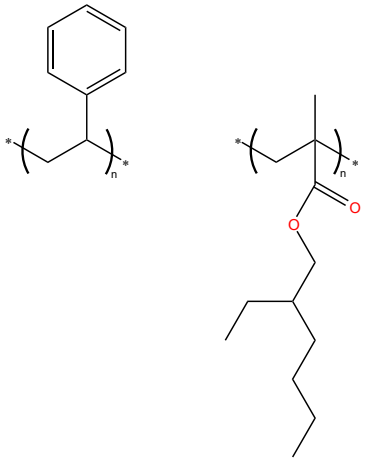

Figure 3.1.1: Chemical structure of poly(styrene) (PS) on the left, and of poly(2-ethyl-hexyl methacrylate) (PEHMA) on the right.

One might be intrigued by the choice of PEHMA as the second polymer. The literature predominantly focuses on PS and poly(methyl methacrylate) PMMA systems, but PMMA's glass transition temperature is comparable to that of PS, making it difficult to distinguish between the two when examining thermal properties. Figure 3.1.2 proves that increasing the length of the aliphatic chain can lower the glass transition temperature. However, this alteration also affects the polarity of the molecule, and it is expected that by increasing the aliphatic chain the polarity will decrease from PMMA to poly(octyl methacrylate). Therefore, although poly(butyl methacrylate) (PBMA, $n = 4$) already has a T_g about 80°C lower than that of PS, to avoid a possible compatibility of PS and PBMA due to their similar polarity [31], it was decided to use PEHMA.

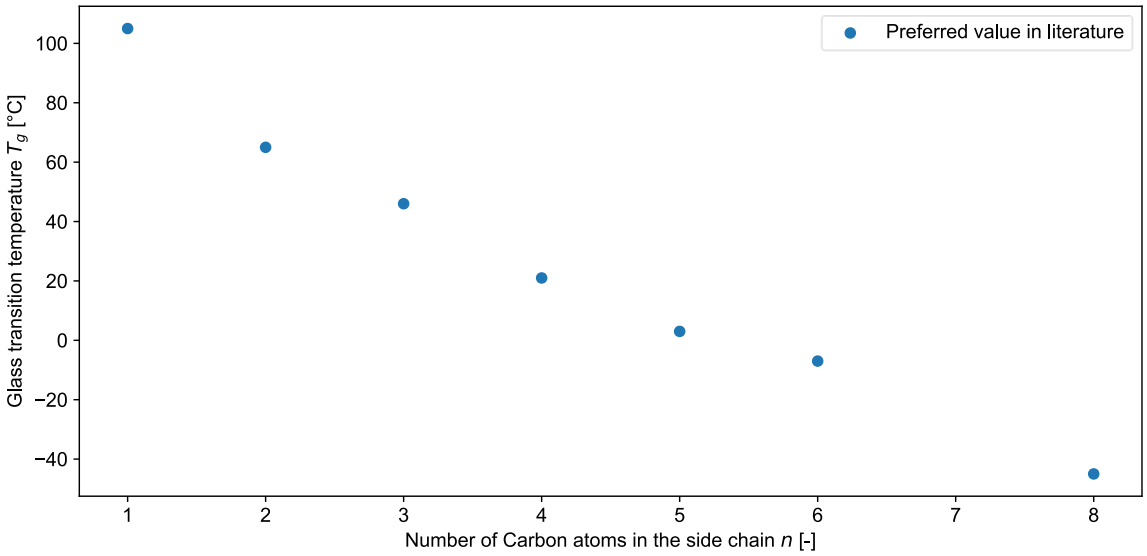

Figure 3.1.2: Glass transition temperature for different poly(n-alkyl methacrylate). The values shown are taken from polymer databases [32, 33].

Section 3.2 Vitrimer Precursor Synthesis and Cross-linking Agent (CLA)

The objective of this section is to provide a comprehensive overview of the molecular structures and synthesis procedures required for the base molecules utilized in the preparation of vitrimer materials. In order to create a vitrimer, it is necessary to functionalize the polymer chains. This process entails modifying the base polymer to incorporate functional groups into the backbone of the chain. This is accomplished through a RAFT co-polymerization process, resulting in the formation of functionalized polymer chains, referred to as "precursors". The presence of functional groups enables the polymer chains to connect to one another via a cross-linking agent.

3.2.1 Synthesis of Poly(styrene)-based Vitrimer Precursor (PS-p)

A precursor for a poly(styrene)-based vitrimer is synthesized through a RAFT co-polymerization process, with a selected functionalization rate of 0.1. The synthesis process is depicted in Figure 3.2.1.

3.2.2 Synthesis of Poly(2-ethyl hexyl methacrylate)-based Vitrimer Precursor (PEHMA-p)

A precursor for a poly(2-ethyl hexyl methacrylate)-based vitrimer is synthesized through a RAFT co-polymerization process, with a selected functionalization rate of 0.1. The synthesis process is depicted in Figure 3.2.2.

NOTE

The synthesis processes were carried out by Ibrahim Göde, as part of his PhD project in the group of Professor Renaud Nicolaÿ at ESPCI Paris.

3.2.3 Cross-linking Agent (CLA)

To connect two polymer chains through their functional groups, a cross-linking agent is required. The cross-linking agent used in this study is 1,4-bis(4-methyl-1,3,2-dioxaborolan-2-yl)benzene, which will be referred to as the cross-linking agent (CLA) throughout this work. The molar mass is $M = 246$ g/mol. The chemical structure of this molecule is illustrated in Figure 3.2.3. The compound identification number of the CLA is CID 140774742.

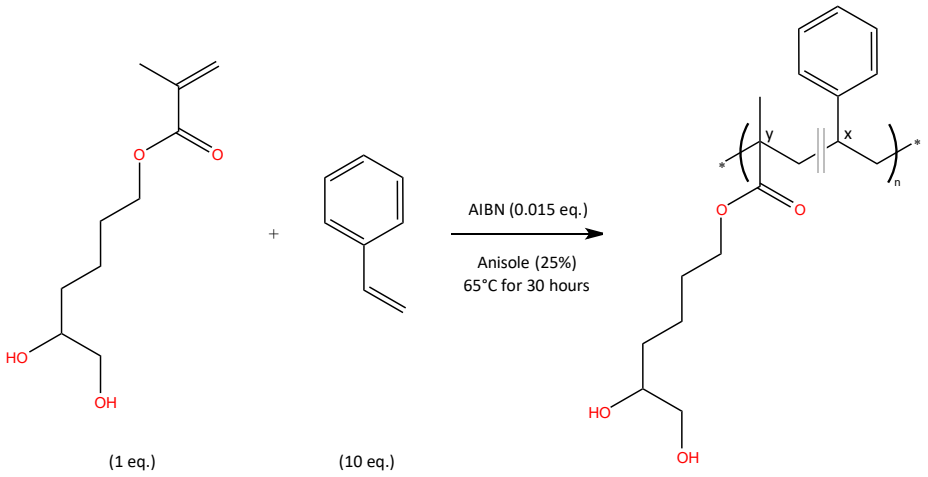

Figure 3.2.1: RAFT synthesis scheme of the poly(styrene) vitrimer precursor (PS-p). The "monomer" unit has an average molar mass of M = 115 g/mol.

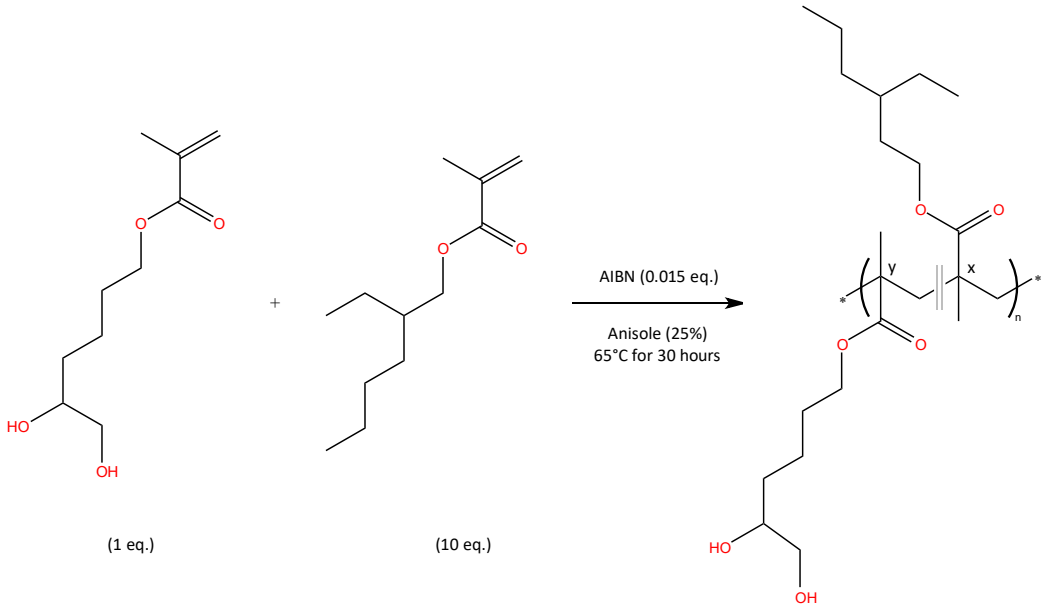

Figure 3.2.2: RAFT synthesis scheme of the poly(2-ethyl hexyl methacrylate) vitrimer precursor (PEHMA-p). The "monomer" unit has an average molar mass of M = 198 g/mol.

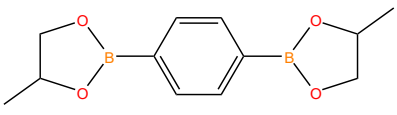

Figure 3.2.3: Chemical structure of the crosslinking agent molecule (CID = 140774742).

Section 3.3 Vitrimer Sample Preparation

The objective of this section is to present the procedure developed to prepare the vitrimer materials used in this study. The process entails dissolving the precursor molecules in a suitable solvent, followed by the addition of a precise amount of cross-linking agent to the solution. This agent can connect the polymer chains together via the functional groups. The amount added is carefully controlled to regulate the cross-linking ratio, denoted as α. This meticulous process results in the creation of a chemical network, which ultimately yields the desired vitrimer material. Additionally, the molecular structures of the vitrimer material obtained are illustrated to facilitate a better understanding of the process.

3.3.1 Preparation Procedure for a Cross-linking Agent Solution

Prior to commencing the vitrimer preparation, it is important to prepare a solution of 6 mL with a concentration of 0.2 mol/L of cross-linking agent (CLA), with THF as a solvent.

3.3.2 Preparation Procedure for a Vitrimer Material

The preparation of a vitrimer is performed in solution with THF as solvent. In the following procedure, the desired mass of vitrimer is noted m. Often, the prepared mass is $m = 250$ mg and the values presented in this procedure are calculated based on this amount. The entire procedure is performed at room temperature.

1) Measure out 250 mg of vitrimer precursor and place it in a 25 mL transparent vial.
2) Add 1.5 mL of THF to the vial and securely close it.
3) Place the vial on a magnetic stirrer and set it to 300 rpm.
4) Allow the precursor to dissolve completely, which should take approximately 30 minutes.
5) For a PS-based vitrimer material:
   For a 20% cross-linking ratio, open the vial and insert 110 µL from the cross-linking agent solution. For a 10% cross-linking ratio, add 55 µL of the solution instead.
   For a PEHMA-based vitrimer material:
   For a 20% cross-linking ratio, open the vial and insert 63 µL from the cross-linking agent solution. For a 10% cross-linking ratio, add 32 µL of the solution instead.

6) Wait for approximately 15 minutes, then open the vial and reduce the mixing speed to 100 rpm.
7) Allow the solvent to evaporate for 48 hours.
8) Recover the vitrimer material.

WARNING

It is imperative that the vial is securely fixed to the plate. During step 6, there is a significant increase in viscosity, and if the vial is not well fixed, the magnetic bar may dislodge the vial, causing it to be ejected from the plate. Therefore, it is crucial to ensure that the vial is firmly secured to the plate before proceeding with the experiment.

The molecular structures of the materials PEHMA-v and PS-v are depicted in Figures 3.3.1 and 3.3.2, respectively.

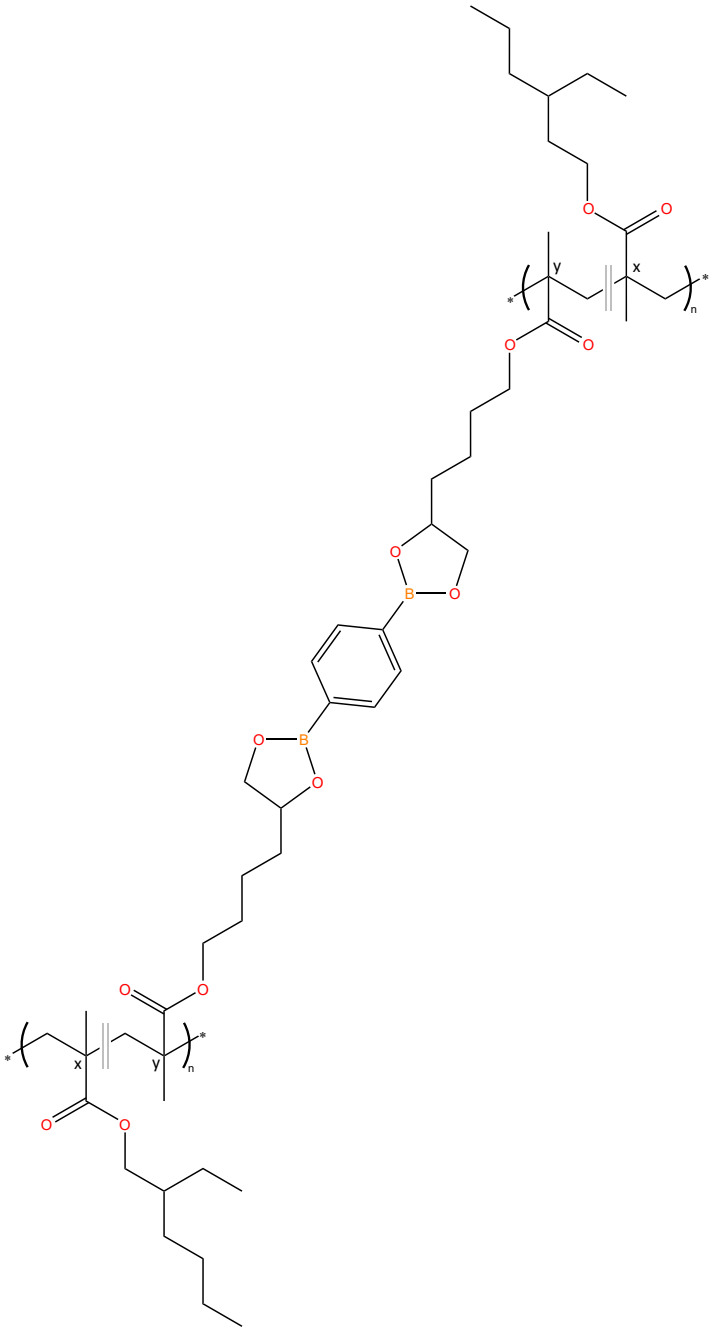

Figure 3.3.1: Chemical structure of the PEHMA-based vitrimer (PEHMA-v). The crosslinker is positioned at the centre, linking two polymer chains on either side.

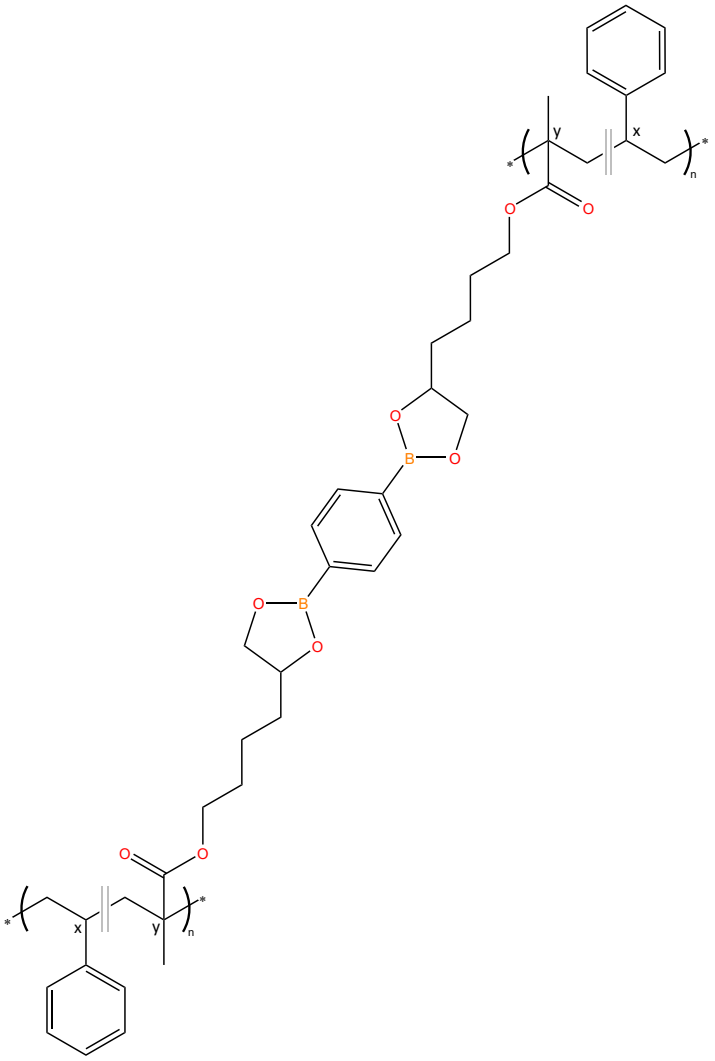

Figure 3.3.2: Chemical structure of the PS-based vitrimer (PS-v). The crosslinker is positioned at the centre, linking two polymer chains on either side.

Section 3.4 Blend Sample Preparation

The purpose of this section is to outline the procedure developed for the preparation of poly(styrene) (PS) and poly(2-ethyl hexyl methacrylate) (PEHMA) blends. The goal is to produce films that can be utilized for the study of surface properties through the use of scanning probe microscopy techniques. Two distinct samples are prepared: one through solvent casting and the other through bulk preparation. The objective is to determine whether the preparation method and the use of a solvent have any impact on the compatibility of these two polymers.

3.4.1 PS (Total Energies) [80 wt.%] and PEHMA (90,000 g/mol) [20 wt.%] (solvent casted)

The process involves dissolving and mixing the two compounds in a solution of tetrahydrofuran (THF). This solution is then carefully poured into a Teflon mold to create a film. The detailed procedure is outlined below:

1) Measure out 2,000 mg of industrial poly(styrene) and place it into a 25 mL transparent vial.
2) Measure out 500 mg of poly(2-ethyl hexyl methacrylate) and place it into the same vial.
3) Add 15 mL of THF to the vial and securely close it.
4) Place the vial on a magnetic stirrer and set it to 300 rpm.
5) Allow the compounds to dissolve completely, which takes approximately 1 hour.
   → The solution should be translucid with a slight white hue.

Once the blend is prepared, it is possible to form a film using an 80 mm diameter circular Teflon mould.

1) Slowly pour the contents into the mould.
2) Wait 48 hours for the solvent to evaporate.
3) Recover the film.

3.4.2 PS (Total Energies) [80 wt.%] and PEHMA (90,000 g/mol) [20 wt.%] (in bulk)

The process involves the manual mixing of two components with the aid of a spatula. Small solid pieces are recovered after this step. Then, to prepare a film, a few solid pieces are flattened using a hot press. The detailed procedure is outlined below:

1) Measure out 400 mg of industrial poly(styrene) and place it into a 25 mL transparent vial.
2) Place the opened vial on a heating plate and set the temperature at 200°C.
   → One should note that this is not the actual temperature inside the vial.
3) Wait for the poly(styrene) to become completely liquid-like (approximately 30 min).
4) Measure out 100 mg of poly(2-ethyl hexyl methacrylate) and place it into the vial.
5) Using a spatula, slowly mix the two polymers until a homogeneous white paste is formed.
6) Let the vial to cool down to room temperature (approximately 20 min).
7) Recover the material.

Once the blend is prepared, it is possible to form a film using a hot press.

1) Put a few mg of the recovered material between two poly(imide) sheets (Kapton sheets).
   → This avoids adhesion problem in the following steps and enables an easy recovery of the film.
2) Set the temperature of the hot press at 220°C.
3) Press the material with a pressure equivalent to one metric ton.
4) Perform three cycles of pressure and pressure release.
   → This step helps at removing air bubbles.
5) Cool the film at room temperature for 3 minutes.
6) Recover the film.

The tables below present a comprehensive list and concise summary of each sample prepared within the scope of this study.

Table 3.4.1: List of available base materials.

PS (Total Energies)	Industrial poly(styrene) PS 1160 provided by Total Energies
PEHMA (DP = 450)	Monodisperse PEHMA with DP = 450 (M = 90,000 g/mol).
PEHMA-p (DP = 450)	Monodisperse PEHMA vitrimer precursor with DP = 450 (M = 90,000 g/mol).
PS-p (DP = 450)	Monodisperse PS vitrimer precursor with DP = 450 (M = 50,000 g/mol).

Table 3.4.2: List of vitrimer samples prepared.

PEHMA-v (DP = 450) (α = 10%)	PEHMA-based vitrimer with a 10% crosslinking ratio.
PEHMA-v (DP = 450) (α = 20%)	PEHMA-based vitrimer with a 20% crosslinking ratio.
PS-v (DP = 450) (α = 10%)	PS-based vitrimer with a 10% crosslinking ratio.
PS-v (DP = 450) (α = 20%)	PS-based vitrimer with a 20% crosslinking ratio.

Table 3.4.3: List of samples with polymer blends prepared.

Blend 1	PS (Total Energies) [80 wt.%] and PEHMA (DP = 450) [20 wt.%] (solvent casted).
Blend 2	PS (Total Energies) [80 wt.%] and PEHMA (DP = 450) [20 wt.%] (sample prepared in bulk).

Section 3.5 Differential Scanning Calorimetry Experimental Method

The aim of this section is to describe the experimental method used to determine the thermal properties of the samples prepared in the context of this project.

3.5.1 Equipment Configuration

Differential Scanning Calorimetry (DSC) analyses are performed on the samples investigated in order to determine the glass transition temperatures. The equipment used is a DSC Mettler Toledo AG204 Delta Range. All samples are heated and cooled down at a rate of 20°C/min to enhance the visibility of transitions. Furthermore, to maintain sample stability and prevent thermo-oxidative degradation, all experiments are conducted under an inert atmosphere of nitrogen gas. To ensure accuracy, all experiments are repeated twice.

3.5.2 Procedure

The procedure developed is described below:

1) Maintain temperature at -85°C for 2 minutes.
2) Heat at a rate of 20°C/min until temperature reaches 150°C.
3) Maintain temperature at 150°C for 2 minutes.
4) Cool down at a rate of 20°C/min until temperature reaches -85°C.
5) Maintain temperature at -85°C for 2 minutes.
6) Heat at a rate of 20°C/min until temperature reaches 150°C.

The nitrogen gas is fed at a rate of 5 mL/min during the entire procedure.

The procedure takes approximately 42 minutes.

NOTE

A mass between 5 mg and 10 mg is required for an analysis.

Section 3.6 Gel Permeation Chromatography Experimental Method

The aim of this section is to describe the experimental method used in Gel Permeation Chromatography (GPC) analyses.

The Gel Permeation Chromatography (GPC), a method introduced in 1964 by J. C. Moore [34], allows to measure the molar mass distribution of polymers. A diluted solution of polymer is injected into a set of GPC columns and the eluted fractions are recorded with a concentration detector, usually a differential refractive index detector.

The chromatogram obtained by injecting a broad polystyrene (PS) sample can be transformed into a molar mass distribution by converting the time axis (minutes) into molar mass. This can be done by injecting a series of PS standards, having narrow molar mass distributions, and known molar masses, to obtain a calibration curve. For any mathematical distribution it is possible to define averages (moments), which in this case are given by the following formulae [35]:

$$M_n = \frac{\sum_i N_i \cdot M_i}{\sum_i N_i} \tag{3.6.1}$$

$$M_w = \frac{\sum_i W_i \cdot M_i}{\sum_i W_i} = \frac{\sum_i N_i \cdot M_i^2}{\sum_i N_i \cdot M_i} \tag{3.6.2}$$

For this work, the PS (Total Energies) was analysed on Waters GPC instrument in dimethyl formamide (DMF). The injected volume was 0.1 mL, the flow rate was 1 mL/min, and the columns were kept at 35°C. Because the calibration was done with PS standards, the measured average molar masses of the PS (Total Energies) are the absolute values.

Section 3.7 Atomic Force Microscopy Experimental Method

The aim of this section is to describe the experimental method used to determine the surface properties of the samples prepared in the context of this project.

3.7.1 Microscope Configuration

The surface properties of the samples being studied are analysed using a Bruker Dimension Icon Atomic Force Microscope, equipped with ScanAsyst technology. The mode utilized for this analysis is Peak Force Tapping Quantitative Nanoscale Mechanical Characterization (PFT-QNM). To conduct this analysis, a reference cantilever with a spring constant of 48.87 N/m and a tip radius of 34 nm has been used.

3.7.2 Photodetector Relative Position

The first step is to confirm that the laser reflection on the cantilever is correctly positioned at the centre of the photodetector. Vertical and horizontal shifts of the photodetector are applied to ensure this.

3.7.3 Photodetector Amplitude Sensitivity Calibration

The photodetector amplitude sensitivity is determined by using a reference sample made of sapphire. The amplitude sensitivity of the photodetector is determined to be 64.51 nm/V ± 4.35 nm/V.

3.7.4 Peak Force Tapping Amplitude Sensitivity Calibration

To determine the peak force amplitude sensitivity, tests are conducted at three different frequencies: 0.5 kHz, 1.0 kHz, and 2.0 kHz. The drive amplitude is set at 50 nm, and the peak force set point is set at 0.1 V.

After conducting the tests, the following values for peak force tapping sensitivity are obtained:

- 695.134 nm/V for 0.5 kHz
- 694.520 nm/V for 1.0 kHz
- 714.964 nm/V for 2.0 kHz

3.7.5 Scanning Experiment

After unloading the sapphire sample, the sample of interest is carefully placed under the microscope. To ensure accurate and reliable results, measurements are conducted at various locations. Initially, zones of 30 µm x 30 µm are scanned. If a particular zone piques interest, it is gradually reduced to 10 µm x 10 µm, 3 µm x 3 µm, or even smaller to focus on a specific feature of the sample. The typical frequency utilized is either 1.0 kHz or 2.0 kHz.

Section 3.8 Rheometry Experimental Method

The aim of this section is to describe the experimental method used to determine the viscoelastic properties of the samples prepared in the context of this project.

3.8.1 Rheometer Configuration

All rheological experiments are performed with an Advanced Rheometric Expansion System (ARES) with an 8 mm diameter disc in plate-plate geometry configuration.

3.8.2 Sample Loading

At the beginning of each test, it is important that the equipment is cautiously cleaned to ensure accurate and reliable results. The temperature is then set to the desired highest temperature for the initial experiment. The zero fixture is performed at this specific temperature. The sample is loaded afterwards. It is necessary to allow the material to relax for approximately 15 minutes. To maintain sample stability and prevent thermo-oxidative degradation, all experiments are conducted under an inert atmosphere of nitrogen gas.

3.8.3 Dynamic Strain Sweep Experiment

In a dynamic strain sweep experiment, the sample is subjected to a sinusoidal strain wave with varying amplitudes, and the resulting stress is measured. This technique allows to establish the limit of the linear regime of deformation for the material. The experiment is conducted at the highest available frequency of 100 rad/s, for strains ranging from 0.1% to 100%. It is important to mention that the test is interrupted as soon as a slight decrease in the storage modulus is observed, in order to avoid entering the non-linear regime.

Additionally, this technique ensures that the sample is properly fixed in the rheometer. If noise is observed instead of a plateau for small strain amplitudes, it might indicate that there is a poor contact between the sample and the parallel plates or that the transducer used is not appropriate. This problem can be resolved by reducing the gap or by changing the transducer type. To provide a better understanding of the issue, an example is illustrated in Figure 3.8.1.

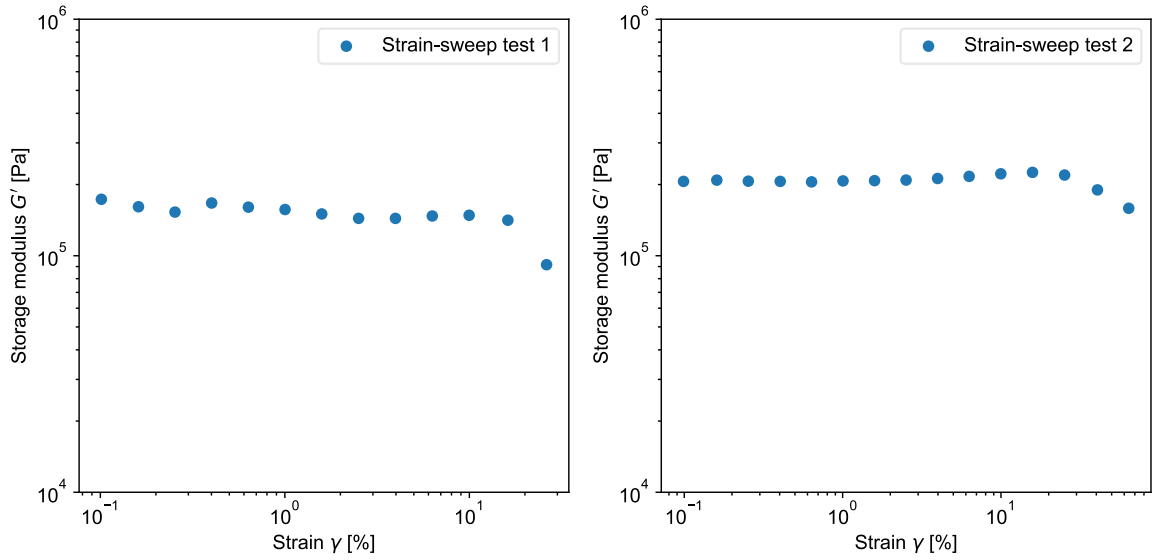

Figure 3.8.1: Comparison of two dynamic strain sweep tests for the sample of PS (Total Energies) performed at 160°C and 100 rad/s. The plot on the left presents noise in the range of small strain amplitudes. This problem is solved be reducing the gap between the parallel plates and therefore by slightly compressing the sample.

To ensure accurate results, a dynamic strain sweep test can be performed at each temperature. However, this method can be time-consuming and may result in the nitrogen tank running out, compromising some measurements. An alternative approach is to perform the dynamic strain sweep at the lowest desired temperature, as the linear regime is valid for all higher temperatures. However, this approach may result in the strain amplitude applied being too small for these higher temperatures, leading to very small stresses being measured and introducing noise in the experimental data. To overcome these limitations, a combination of both approaches is adopted in this work.

3.8.4 Dynamic Frequency Sweep Experiment

If the experimental conditions are suitable, one can perform a dynamic frequency sweep experiment. A comprehensive explanation is provided in Section 2.1 about the Small Amplitude Oscillatory Shear (SAOS) experiment utilized in this project. This method is employed to determine the storage and loss moduli of the investigated materials. The frequency range spans from 100 rad/s to 0.01 rad/s.

3.8.5 Sample Unloading

To prevent any damage to the rheometer, it is important to exercise caution when unloading the sample. The unloading process should be carried out at a sufficiently high temperature to allow the material to flow and not restrict the transducer. This approach ensures that the sample can be removed without applying excessive axial forces on the transducer while separating the parallel plates.

Part 4 Experimental Results and Discussions

The main properties of raw materials are measured by Differential Scanning Calorimetry (DSC) and Gel Permeation Chromatography (GPC). Atomic Force Microscopy (AFM) is applied to blends. Further, each sample undergoes a rheological study, which is a characterization technique that effectively connects the molecular structures of the polymers with their macroscopic mechanical properties.

Section 4.1 Differential Scanning Calorimetry

The purpose of this section is to present the results obtained using the Differential Scanning Calorimetry analysis on the studied samples.

Differential scanning calorimetry (DSC) analyses are performed on the samples PS (Total Energies), PS-v (50,000 g/mol) (α = 20%) and PEHMA (90,000 g/mol) in order to determine the glass transition temperatures of these materials. The results are illustrated in Figure 4.1.1.

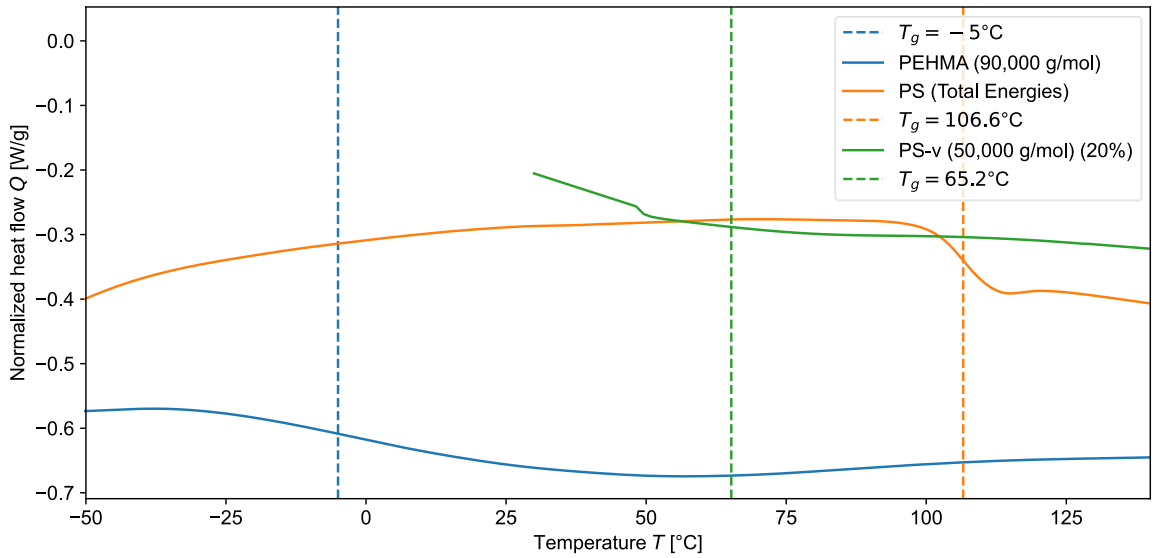

Figure 4.4.1: Normalized heat flows for the samples PS (Total Energies), PS-v (50,000 g/mol) (α = 20%) and PEHMA (90,000 g/mol) as functions of temperature. The values for the glass transition temperatures are marked as vertical dashed lines.

The glass transition temperature of the PS (Total Energies) sample is easily detectable and is determined to be 106.6°C ± 1°C. For PS-v (50,000 g/mol) (α = 20%), the glass transition temperature is determined to be 65.2°C ± 1°C. For the PEHMA (90,000 g/mol) sample, the glass transition temperature is not as apparent and cannot be accurately pinpointed. A value of -5°C ± 5°C is identified, albeit a broad transition range spanning over about 150°C. This observation is confirmed in literature [36]. Nevertheless, this value is retained for the purpose of model implementations.

Section 4.2 Gel Permeation Chromatography

The purpose of this section is to briefly present the results obtained using the Gel Permeation Chromatography analysis on the studied samples.

A gel permeation chromatography (GPC) analysis is performed on the PS (Total Energies) sample to determine the molar mass distribution. This particular sample is polydisperse, making this analysis quite important. A number-average molar mass M_n of 81,450 g/mol, a weight-average molar mass M_w of 200,200 g/mol and a polydispersity of 2.5 are determined.

Section 4.3 Atomic Force Microscopy

This section presents the findings of the atomic force microscopy experiments. The purpose of the experiments is to determine the compatibility of poly(styrene) (PS) and poly(2-ethyl hexyl methacrylate) (PEHMA), and to investigate whether the sample preparation method has any influence on the results. The findings show that PS and PEHMA are not compatible with each other. Distinct surface properties are observed, and nodules are present, regardless of the sample preparation method employed.

4.3.1 PS (Total Energies) [80 wt.%] and PEHMA (90,000 g/mol) [20 wt.%] (solvent casted)

An analysis is conducted on a polymer blend sample, prepared via solvent dissolution described in Section 3.2. The purpose of this analysis is to determine the compatibility between PS and PEHMA. The results reveal the presence of nodules on the surface of the sample, with an approximate diameter of 350 nm. The surface properties of the sample vary significantly, which indicates the presence of two distinct phases: a hard phase of PS and a soft phase of PEHMA, as depicted in Figure 4.3.1. The variation in stiffness on the surface of the sample is clearly visible. To better illustrate this, a profile of the stiffness is extracted from the image and plotted in Figure 4.3.2. The plot shows a sharp interface between the two phases.

4.3.2 PS (Total Energies) [80 wt.%] and PEHMA (90,000 g/mol) [20 wt.%] (in bulk)

An analysis is conducted on a polymer blend sample, prepared via bulk mixing of each component. The purpose of this analysis is to determine the compatibility between PS and PEHMA, and to investigate whether a change in the sample preparation method has any influence on the results. The results reveal the presence of nodules on the surface of the sample, with an approximate diameter of 100 nm. The change in surface properties indicate the presence of two distinct phases: a hard phase of PS and a soft phase of PEHMA, as depicted in Figure 4.3.3. The variation in stiffness on the surface of the sample is also clearly visible. A profile of the stiffness is extracted from a zoom image (see Figure 4.3.4) and plotted in Figure 4.3.5. The plot shows a sharp interface between the two phases.

The information obtained on the interface of the un-compatibilized blends is essential for the ultimate goal of the project. It is important to recall that the research project aims to prove that the vitrimers can play the role of compatibilizers at the interface, which enhances the mechanical properties of recycled polymers.

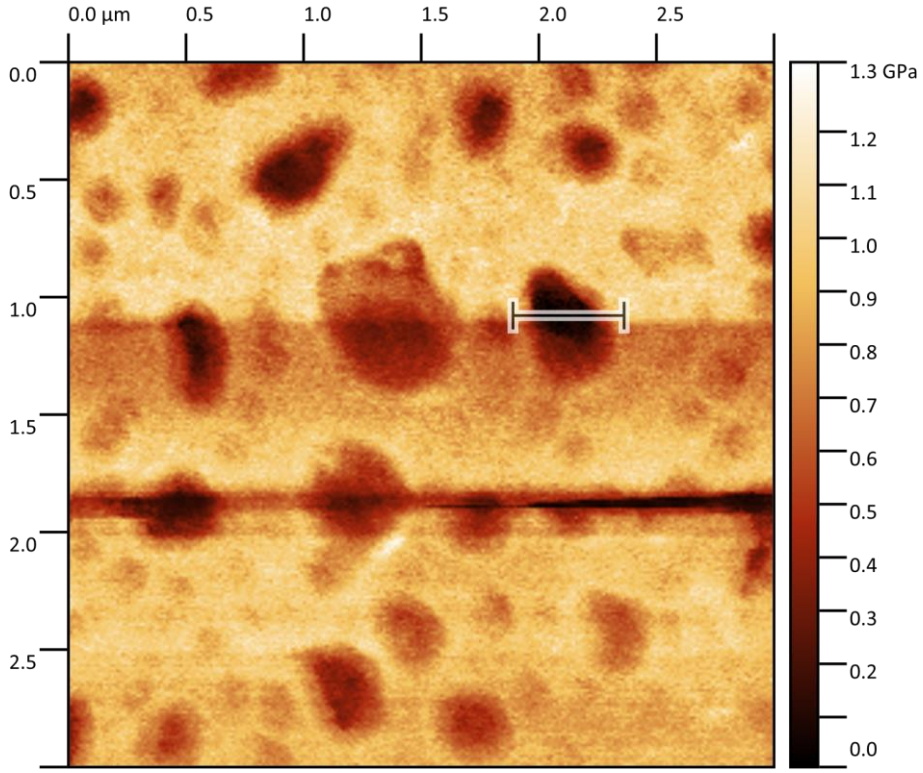

Figure 4.3.1: Surface stiffness on a 3 µm x 3 µm surface of a PS (Total Energies) [80 wt.%] and PEHMA (90,000 g/mol) [20 wt.%] sample prepared in solution. The bar shows the location of the profile in Figure 4.3.2.

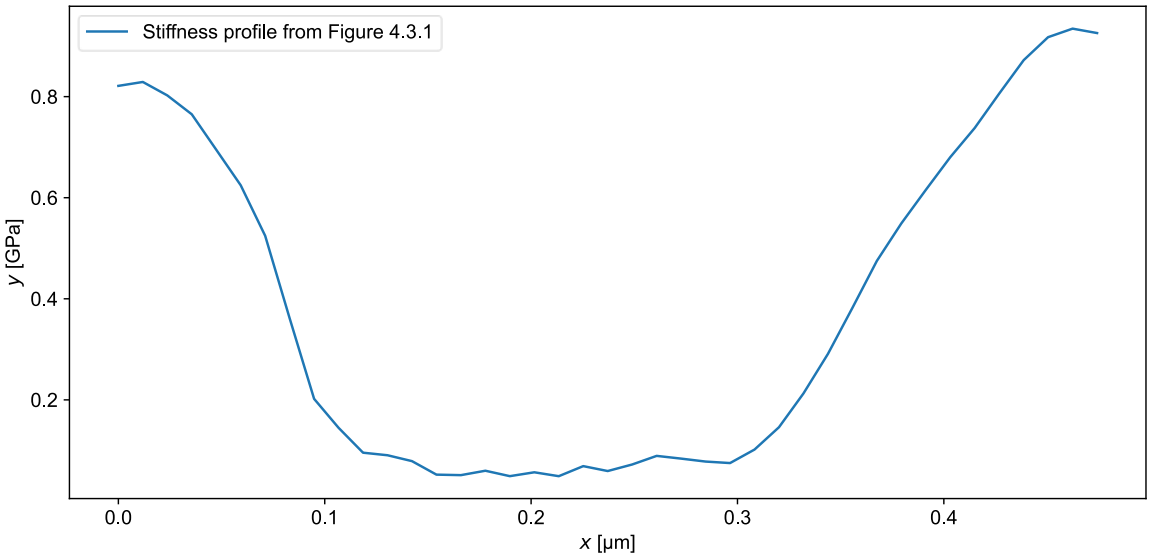

Figure 4.3.2: Stiffness profile from Figure 4.3.1. extracted on a nodule of the sample PS (Total Energies) [80 wt.%] and PEHMA (90,000 g/mol) [20 wt.%] prepared with solvent.

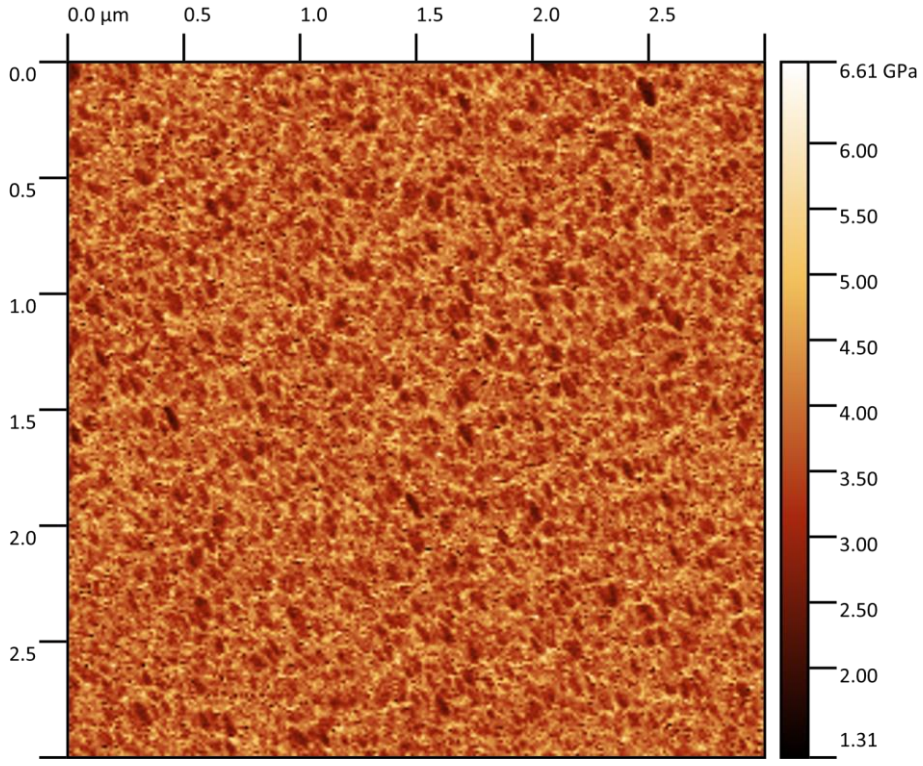

Figure 4.3.3: Surface stiffness on a 3 µm x 3 µm surface of a PS (Total Energies) [80 wt.%] and PEHMA (90,000 g/mol) [20 wt.%] sample prepared without solvent.

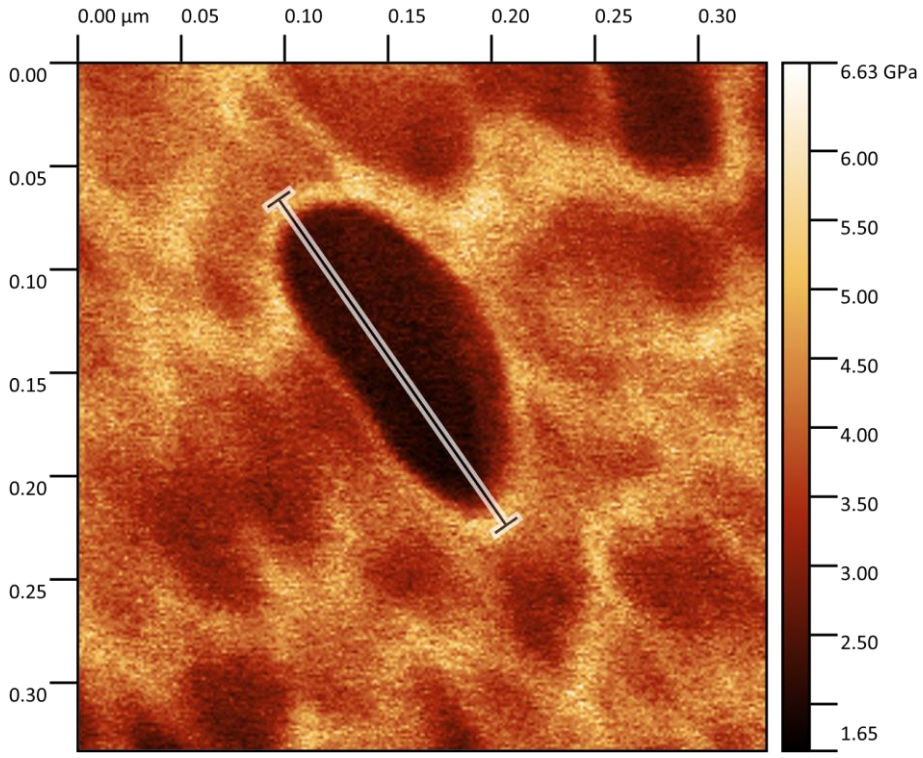

Figure 4.3.4: Surface stiffness on a 33 nm x 33 nm surface of a PS (Total Energies) [80 wt.%] and PEHMA (90,000 g/mol) [20 wt.%] sample prepared without solvent. The bar shows the location of the profile.

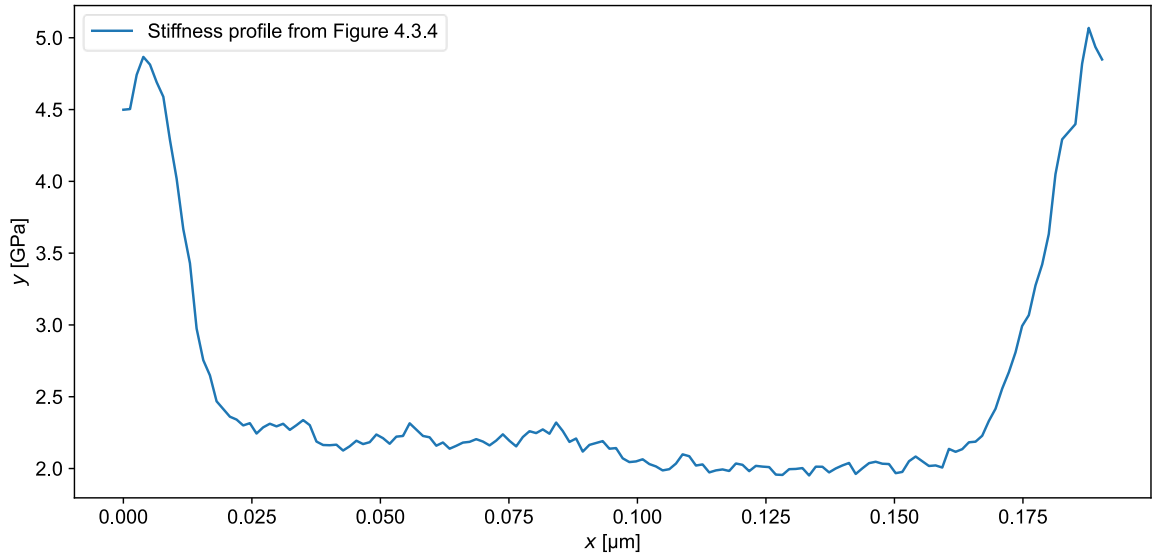

Figure 4.3.5: Stiffness profile from Figure 4.3.4. extracted on a nodule of the sample PS (Total Energies) [80 wt.%] and PEHMA (90,000 g/mol) [20 wt.%] prepared without solvent.

Section 4.4 Rheometry Method Qualification

In this section, the rheological method for measuring the viscoelastic properties is tested on a well-defined sample, before applying it on the investigated materials. The sample used is PS (Total Energies). It serves as a reference sample for verifying the storage and loss moduli using the method described in Section 3.8. The results demonstrate the validity of the obtained values and support the application of the Time Temperature Superposition principle using parameters sourced from literature.

4.4.1 Experimental Measurements

Before determining the viscoelastic properties of vitrimer materials, it is important to ensure that the method employed yields accurate experimental values. To achieve this, several experiments are conducted on a reference sample PS (Total Energies). The viscoelastic properties of different poly(styrene) samples are well-documented, and the experimental data obtained can be compared with data from existing literature.

The experimental data for the PS (Total Energies) sample is illustrated in Figure 4.4.1:

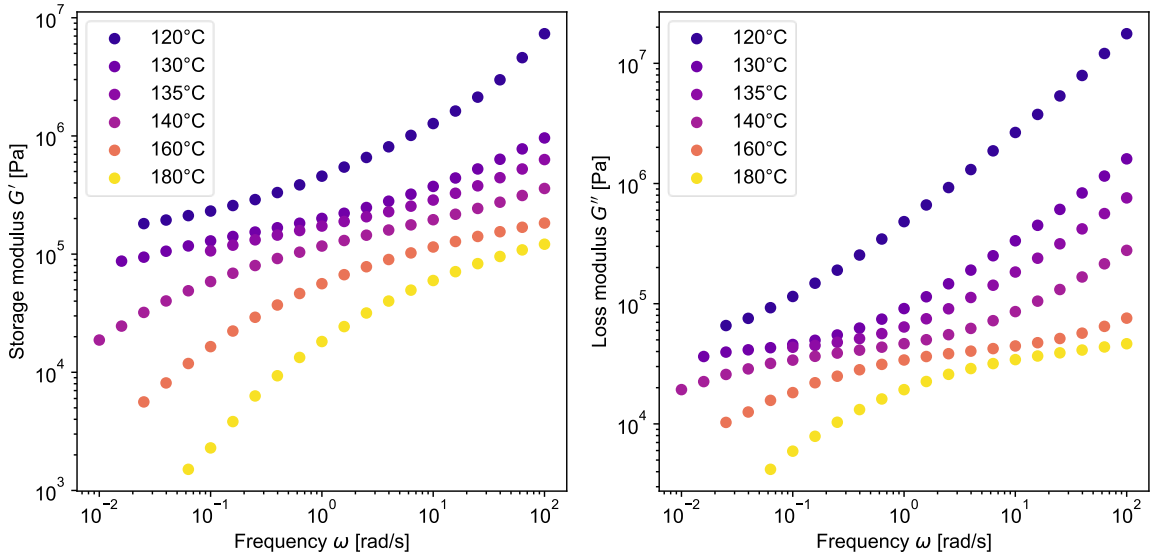

Figure 4.4.1: Experimental data for the storage modulus of the sample PS (Total Energies) from Small Amplitude Oscillatory Shear (SAOS) performed at 120°C, 130°C, 135°C, 140°C, 160°C and 180°C.

4.4.2 Time Temperature Superposition

A method for validating the experimental results is to apply the Time Temperature Superposition (TTS) principle by shifting the data sets. The temperature dependence used is the Williams-Landel-Ferry (WLF) model. By using values for C_1 and C_2, established in literature for a specific reference temperature, the curves should align. To test this approach, two sets of parameters that are commonly used in literature are examined:

$C_1 = 6.74$ and $C_2 = 133.6$ at a reference temperature of 160°C [37]

$C_1 = 8.40$ and $C_2 = 80.0$ at a reference temperature of 130°C [38]

For the vertical shift factors, an empirical expression is used to compute the density of poly(styrene): [38]

$$\rho(T) = 1.2503 - 6.05 \cdot 10^{-4} \cdot T$$

The horizontal and vertical shift factors are illustrated in Figure 4.4.2.

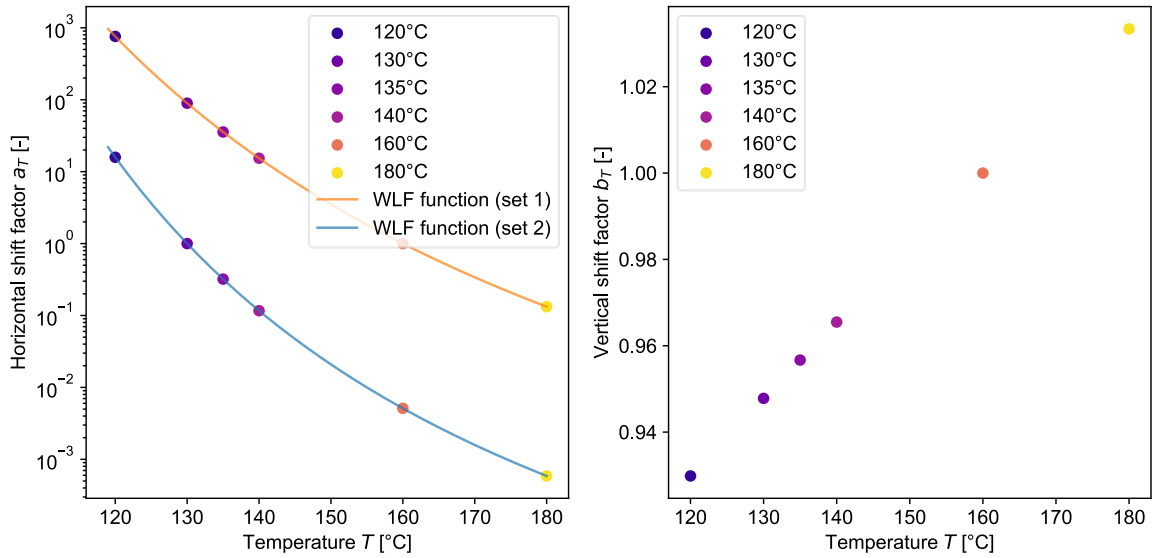

Figure 4.4.2: Horizontal and vertical shift factors for the PS (Total Energies) using the Williams-Landel-Ferry function. The "set 1" refers to $C_1 = 6.74$ and $C_2 = 133.6$ and the "set 2" refers to $C_1 = 8.40$ and $C_2 = 80.0$.

By using the horizontal and vertical shift factors, a master curve can be constructed. The process is exemplified in Figures 4.4.3 and 4.4.4.

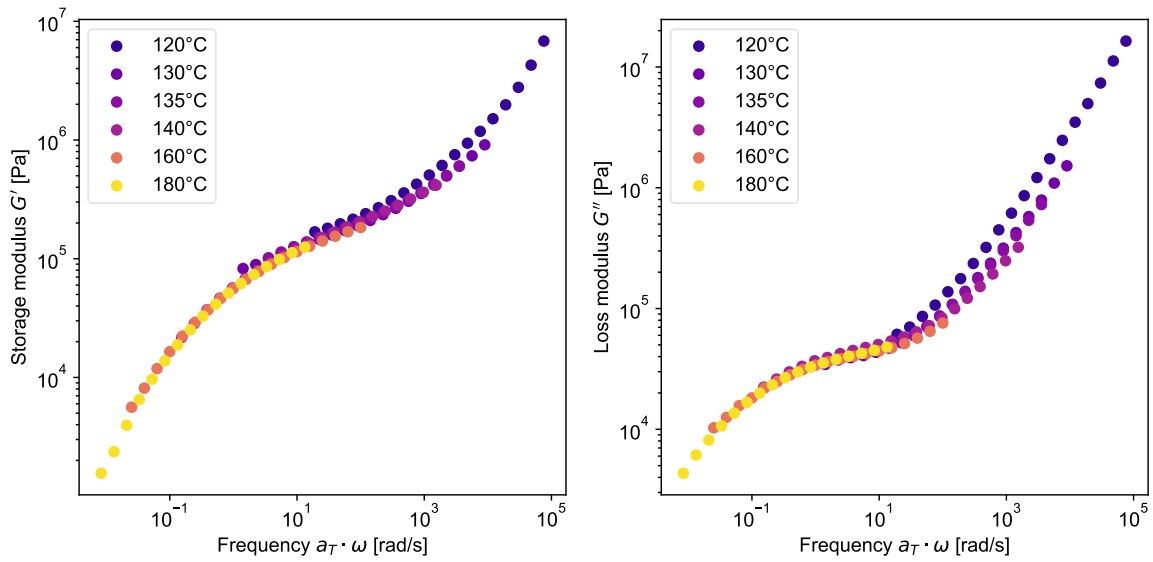

Figure 4.4.3: Master curve of the storage and loss moduli of the sample PS (Total Energies) at a reference temperature of 160°C using the Williams-Landel-Ferry model with $C_1 = 6.74$ and $C_2 = 133.6$.

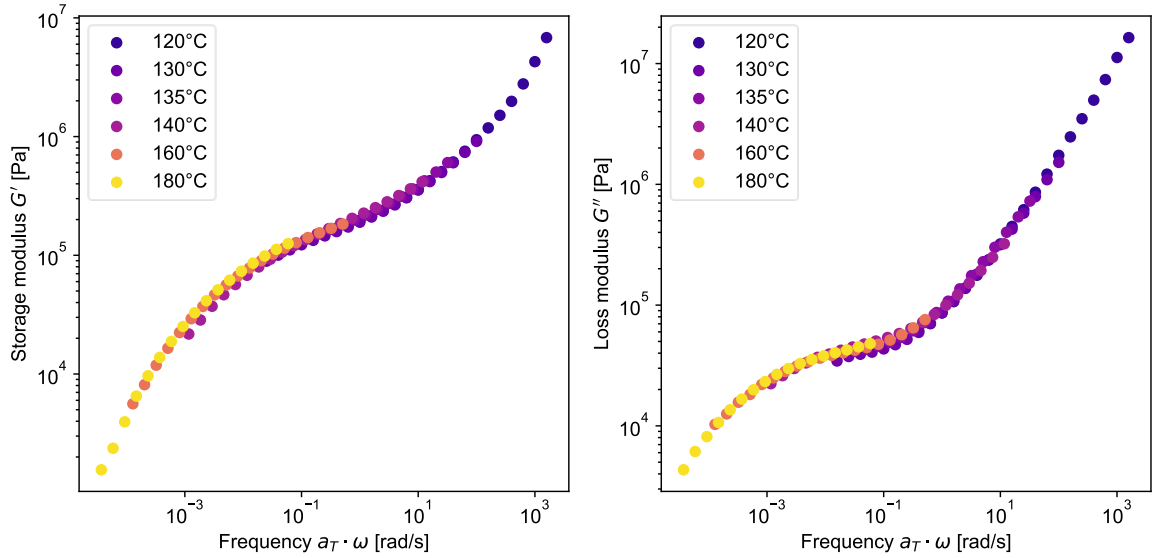

Figure 4.4.4: Master curve of the storage and loss moduli of the sample PS (Total Energies) at a reference temperature of 130°C using the Williams-Landel-Ferry model with $C_1 = 8.40$ and $C_2 = 80.0$.

The experimental data is validated, as a remarkable superposition of the data sets is observed for low frequencies, which correspond to high temperatures. However, a deviation is noticed at high frequencies for the first set of constants. This could be due to the fact that the

experiments are conducted near the glass transition temperature of the material, and some unaccounted effects might take place. Nonetheless, a better superposition is achieved using the second set of constants at a reference temperature of 130°C.

When superposing experimental curves, it is often useful to examine the tangent of the phase angle, $\tan(\delta)$, since the vertical shift coming from experimental issues is cancelled out. This is thus an easy way to work with normalized curves. The $\tan(\delta)$ curves corresponding to each set of parameters are shown in Figure 4.4.5.

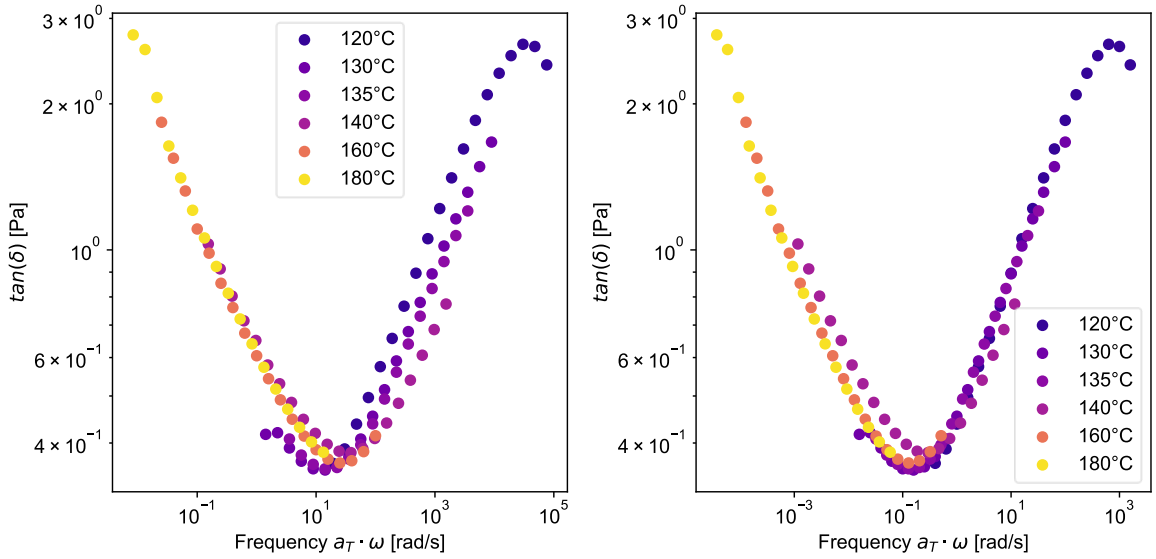

Figure 4.4.5: Master curve of the tan(δ) of the sample PS (Total Energies) based on the first (on the left) or the second (on the right) set of parameters.

The previous observation is verified, and a better superposition is achieved with the second set of parameters. As a result, this set of constants is selected for further implementation in this study.

The Time Temperature Superposition principle is a crucial aspect of the data analysis. By utilizing values extracted from literature, one can confidently assert that the experiments have been conducted with precision and accuracy. This principle serves as a reliable indicator of the validity of the results, providing a solid foundation upon which to build conclusions for the investigation of vitrimers.

Section 4.5 Model Method Qualification

In this section, the rheological model for determining the viscoelastic properties is tested on a well-defined sample, before applying it on the investigated materials. The sample used is PS (Total Energies) and the experimental data is obtained from Section 4.4. The results demonstrate the validity and the correctness of the Time Marching Algorithm, described in Section 2.3.

The Time Marching Algorithm described in Section 2.3 is implemented using Python code. To accurately model the viscoelastic properties of the materials under investigation, it is crucial that the model produces reliable and precise results. To achieve this, the program is used on the master curve of the reference sample PS (Total Energies) determined in Section 4.4. The parameters required for this simulation are clearly defined in literature. For a reference temperature of 130°C, the entanglement plateau level must be set at $2.3 \cdot 10^5$ Pa, the average molar mass between two entanglement points must be set at 14 kg/mol, and the relaxation time of an "entanglement" segment must be set at 0.39 s [39]. In this case, the molar mass of the Kuhn segment is considered as 0.42 kg/mol (four times the molar mass of the monomer unit of styrene).

Additionally, as the polymer sample is polydisperse, a log-normal molar mass distribution is used based on the values obtained in the GPC analysis (see Section 4.2). The log-normal molar mass distribution is built with $M_n = 81{,}450$ g/mol and $M_w = 200{,}200$ g/mol. A set of 100 points is generated. The log-normal molar mass distribution used is illustrated in Figure 4.5.1.

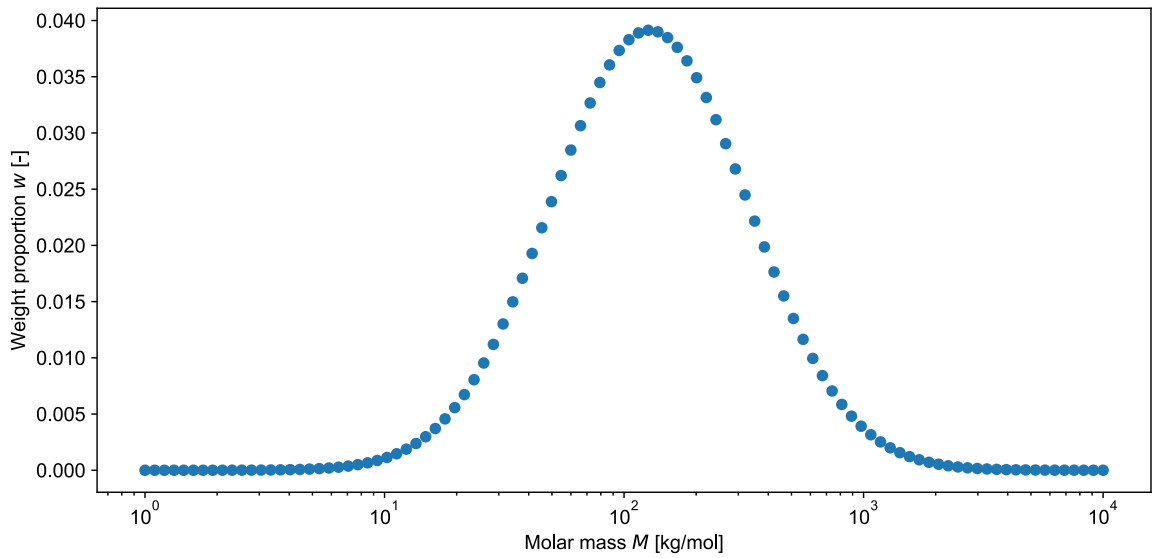

Figure 4.5.1: Log-normal molar mass distribution with the parameters $M_n = 81{,}450$ g/mol and $M_w = 200{,}200$ g/mol.

Using the mentioned parameters and the log-normal molar mass distribution, one can construct the master curves of the storage and loss moduli of the sample PS (Total Energies).

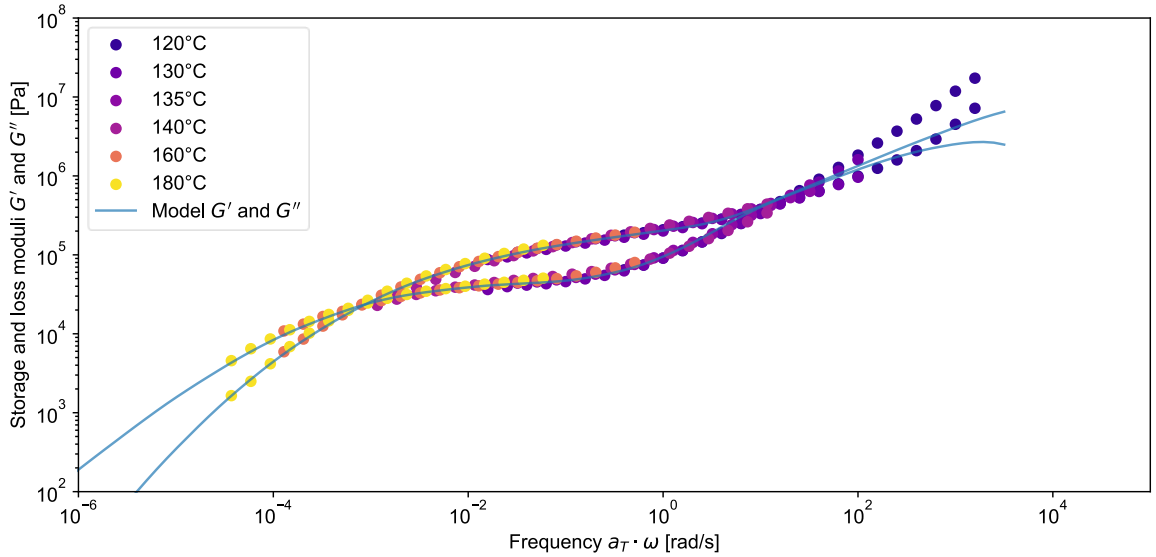

Figure 4.5.2: Storage and loss moduli experimental data with the model predictions for the sample PS (Total Energies) at a reference temperature of 130°C.

The model predictions are in very good agreement with the experimental data. One notices that the curves do not superpose at high frequencies, above 10^2 rad/s, corresponding to low temperatures. This is expected as the relaxation phenomena occurring near the glass transition temperature are not implemented yet. These results validate the implementation of the model.

Section 4.6 Viscoelastic Properties of PEHMA-based Samples

This section describes the rheological experiments performed on the PEHMA-based samples. It is observed that the addition of vitrimers improves the mechanical properties compared to the base material: a rubbery plateau appears in the storage modulus and its value increases with the number of dynamic covalent bonds present in the material. The material is also able to flow at high temperature, enabling its processing. Moreover, the activation energy for flow is estimated using the Arrhenius model.

4.6.1 PEHMA (90,000 g/mol)

As a first step, the base material PEHMA (90,000 g/mol) is characterized using Small Amplitude Oscillatory Shear (SAOS). This sample serves as a baseline for understanding the influence of the addition of dynamic covalent bonds to the material. The experiments are performed at several temperatures in order to build a master curve. The experimental data for this sample is illustrated in Figure 4.6.1.

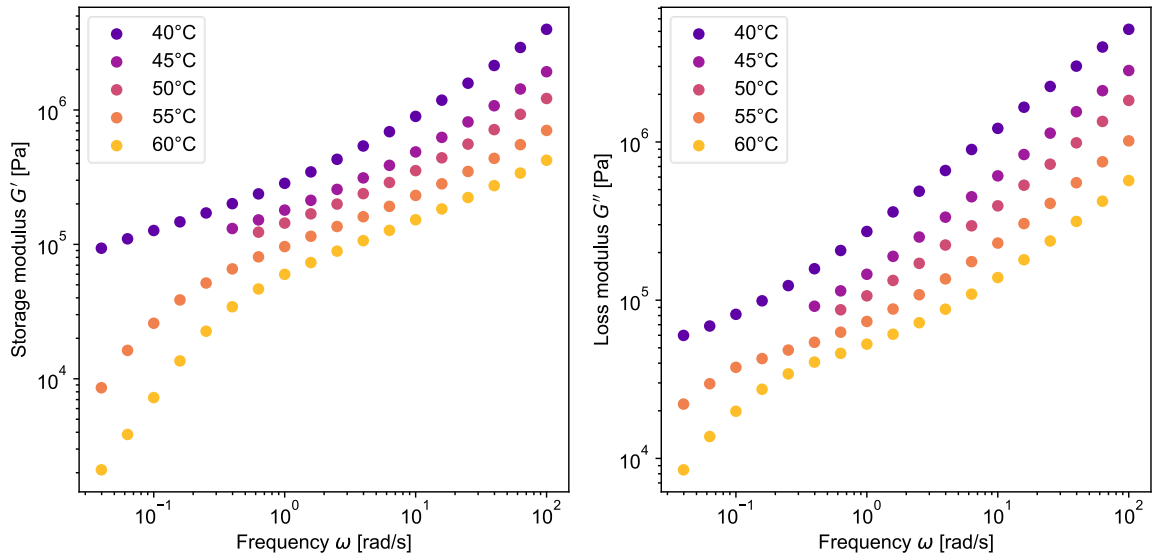

Figure 4.6.1: Experimental data for the storage and loss moduli of the sample PEHMA (90,000 g/mol) from Small Amplitude Oscillatory Shear (SAOS) performed at 40°C, 45°C, 50°C, 55°C, 60°C.

To build the master curve, the Time Temperature Superposition principle is applied. As discussed in Section 4.4, it is important to know the values of C_1 and C_2 in the Williams-Landel-Ferry model to shift the experimental data sets. However, in this case, the values of C_1 and C_2 are not readily available in literature. To overcome this challenge, the ARES software TA Orchestrator is used to optimize the shift factors and generate the most accurate master curve possible. This process ensures that the experimental data sets are appropriately shifted. A low reference temperature of 40°C is selected. Therefore, the high frequencies range i.e., from 10^0 rad/s to 10^2 rad/s, is not shifted. The Williams-Landel-Ferry function is then used to perform a curve fit on the horizontal shift factors. The constants C_1 and C_2 are determined to be 9.0435 and 100.61, respectively, as shown in Figure 4.6.2.

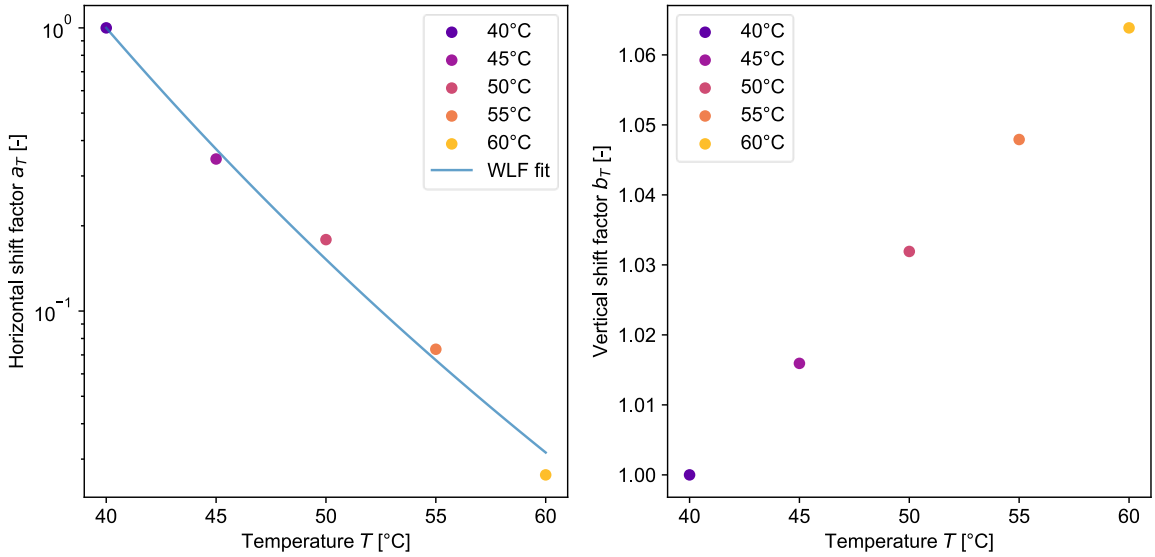

Figure 4.6.2: Horizontal and vertical shift factors for the PEHMA (90,000 g/mol) determined using the ARES software at a reference temperature of 40°C. A Williams-Landel-Ferry (WLF) curve fit is performed on the horizontal shift factors.

The master curve of the sample under investigation can be constructed with the horizontal and vertical shift factors taken from the ARES software. The resulting curves of the storage and loss moduli are illustrated in Figure 4.6.3.

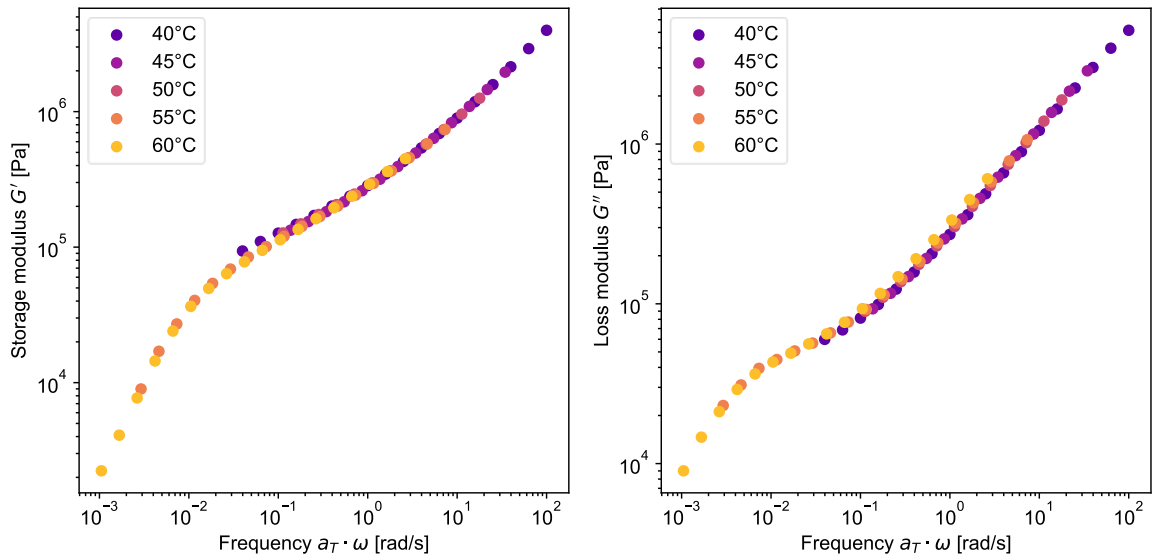

Figure 4.6.3: Master curve of the storage and loss moduli of the sample PEHMA (90,000 g/mol) using the ARES software shift factors at a reference temperature of 40°C.

A good superposition of the experimental data sets is observed for all available frequencies. Therefore, the values $C_1 = 9.0435$ and $C_2 = 100.61$ are considered valid for the investigated material.

An observation of the storage modulus highlights that the polymer chains are not very entangled. Indeed, an entanglement plateau is not observed, but there is a distinguishable "shoulder" (between 10^{-1} rad/s and 10^{0} rad/s) suggesting the level of the entanglement plateau is located around 10^{5} Pa. In the low frequencies range, between 10^{-3} rad/s and 10^{-2} rad/s, the terminal regime is observed, corresponding to the flow of the material. To confirm the values of the entanglement plateau and to understand the underlying molecular properties of the material, the Time Marching Algorithm can be applied to the master curve.

Several sets of parameters are tested to have a good fit of the model. The best fit is found using 0.6 kg/mol for the molar mass of the Kuhn segment, $2 \cdot 10^{5}$ Pa for the entanglement plateau level, 30 kg/mol for the average molar mass between two entanglement points, and 2.5 s for the relaxation time of an "entanglement" segment. The model curve and the experimental master curves are illustrated in Figure 4.6.4.

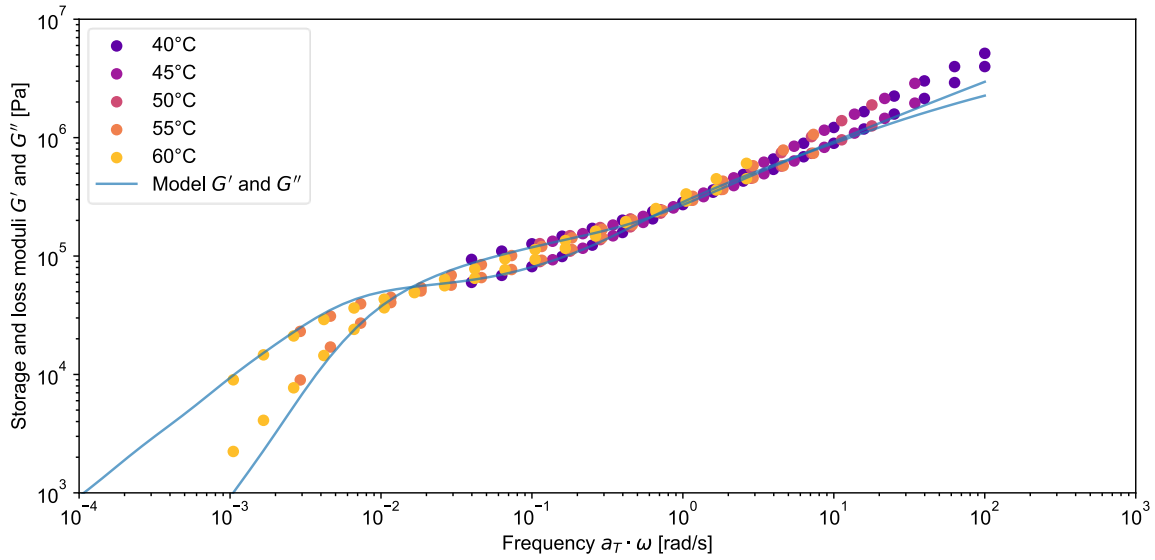

Figure 4.6.4: Master curves of the storage and loss moduli with the model predictions for the sample PEHMA (90,000 g/mol) at a reference temperature of 40°C.

The values found using the model fit confirm that the polymer chains are not heavily entangled. In fact, by calculating the average number of entanglements per chain, it is found that it is only 90 [kg/mol] / 30 [kg/mol] = 3, which is relatively low. Additionally, one can see that the model predictions and the experimental data do not align at high frequencies i.e., above 10^0 rad/s. This is due to the influence of the glass transition temperature. Although the experiments are conducted at a temperature of 40°C, which is significantly higher than the determined glass transition temperature of -5°C (ΔT = 45°C) in the DSC experiments, it is important to note that the transition spans a wide range of temperatures (150°C between -30°C and 120°C).

4.6.2 PEHMA-v (90,000 g/mol) (α = 10%)

The vitrimer PEHMA-v (90,000 g/mol) containing 10% of crosslinkers (α = 10%) is characterized using Small Amplitude Oscillatory Shear (SAOS). This is the first sample containing dynamic covalent bonds in its structure. The experiments are performed at several temperatures to build a master curve. The experimental data for this sample is illustrated in Figure 4.6.5.

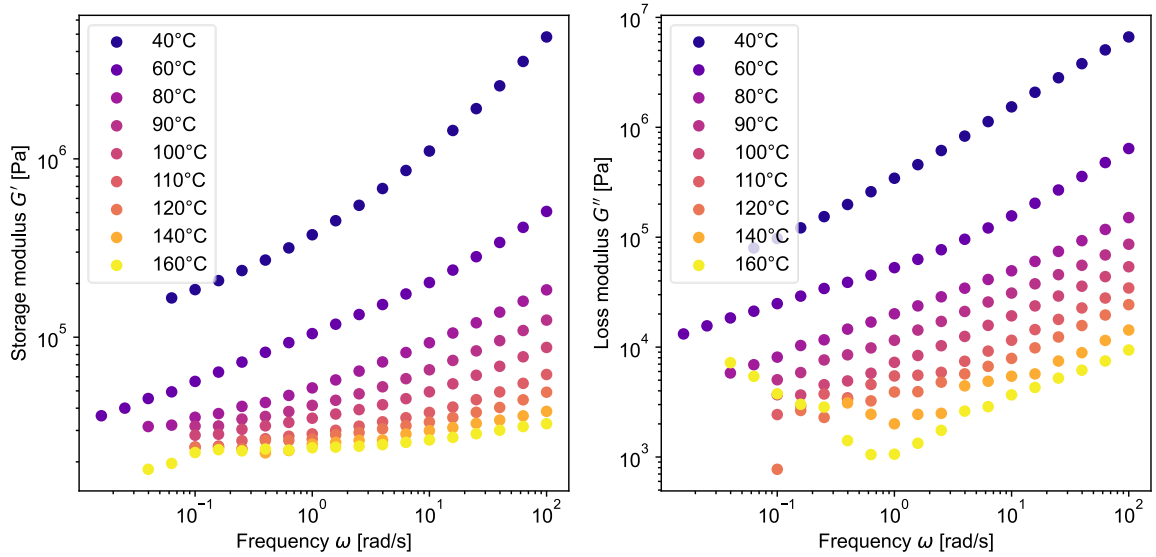

Figure 4.6.5: Experimental data for the storage and loss moduli of the sample PEHMA-v (90,000 g/mol) (α = 10%) from Small Amplitude Oscillatory Shear (SAOS) performed at 40°C, 60°C, 80°C, 90°C, 100°C, 110°C, 120°C, 140°C and 160°C.

A master curve can be constructed using the Time Temperature Superposition principle. The refence temperature is set at to 40°C, as for the previous sample PEHMA (90,000 g/mol). The Williams-Landel-Ferry model is applied to the experimental curves. The values used for the horizontal shift factors are set to $C_1 = 9.0435$ and $C_2 = 100.61$, found for the previous sample. This is acceptable as both materials share the same molecular chemistry and thermal properties. The vertical shifts are set to 1. This is also an acceptable approximation as Figure 4.6.2 shows that the vertical shift factors range between 1 and 1.07. The master curves are shown in Figure 4.6.6.

A superposition of the experimental data sets is observed at low frequencies, below 10^{-5} rad/s, for the storage modulus. However, there is a noticeable lack of superposition in the intermediate frequencies range, between 10^{-5} rad/s and 10^{1} rad/s, suggesting there is a process that is not considered. At high frequencies, or above 10^{1} rad/s, the curves seem to converge. This is more visible in the loss modulus.

The Arrhenius model can enhance the superposition of the curves by taking into account the activation energy for flow. Notably, an activation energy of $E_a = 25{,}000$ J/mol significantly improves the superposition in the storage modulus for all frequencies, as depicted in Figure 4.6.7. One notices however a discontinuity appearing in the master curve of the loss modulus, at 10^{-1} rad/s. At these high frequencies, the exchange dynamics of the dynamic covalent bonds is too slow to show any temperature dependence, and the influence of temperature is only dependent on the segmental dynamics of the chain backbone (i.e., WLF). In the intermediate regime of frequency, as both processes are of equal importance and as they have a different temperature dependence, thermo-rheological complexity is observed.

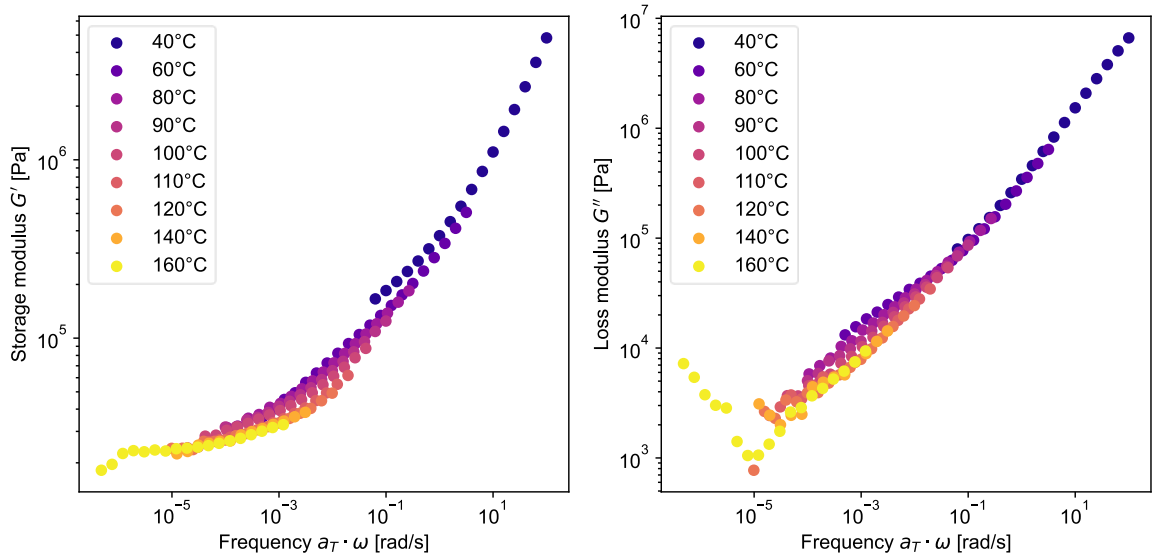

Figure 4.6.6: Master curve of the storage and loss moduli of the sample PEHMA-v (90,000 g/mol) (α = 10%) using the Williams-Landel-Ferry model with $C_1 = 9.0435$ and $C_2 = 100.61$.

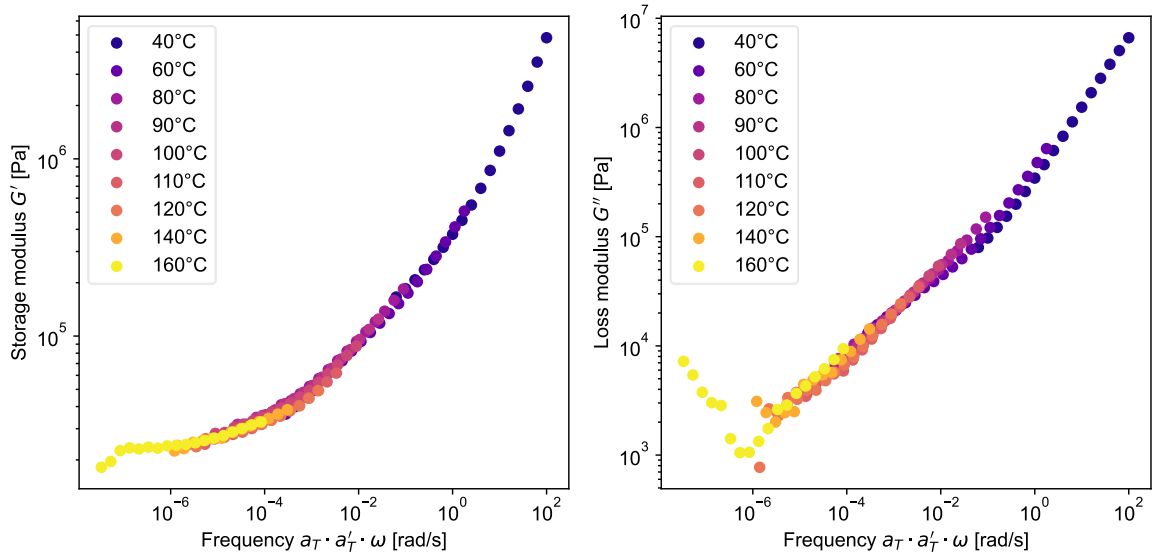

Figure 4.6.7: Master curve of the storage and loss moduli of the sample PEHMA-v (90,000 g/mol) (α = 10%) using the Williams-Landel-Ferry model with $C_1 = 9.0435$ and $C_2 = 100.61$ and the Arrhenius model with an activation energy of flow $E_a = 25{,}000$ J/mol.

In the experimental data, one sees that a new plateau emerges in the storage modulus in the frequency range around 10^{-6} rad/s, reaching a level above $10^4 \cdot$ Pa. This observation is supported by the presence of a minimum in the loss modulus at 10^{-6} rad/s, which is noticeable in the curve corresponding to 160°C (in yellow). Interestingly, this plateau was not present in the previous material, PEHMA (90,000 g/mol), suggesting the formation of a sparsely-crosslinked network, as expected with the low crosslinking ratio of α = 10%.

To gain a better understanding of the impact of covalent dynamic bonds, it is interesting to visualize the horizontal shift factors both with and without the Arrhenius model added. This approach can provide valuable insights into the behaviour of these bonds. Additionally, it allows for a more comprehensive analysis of the system under investigation. The experimental and theoretical shift factors are shown in Figure 4.6.8.

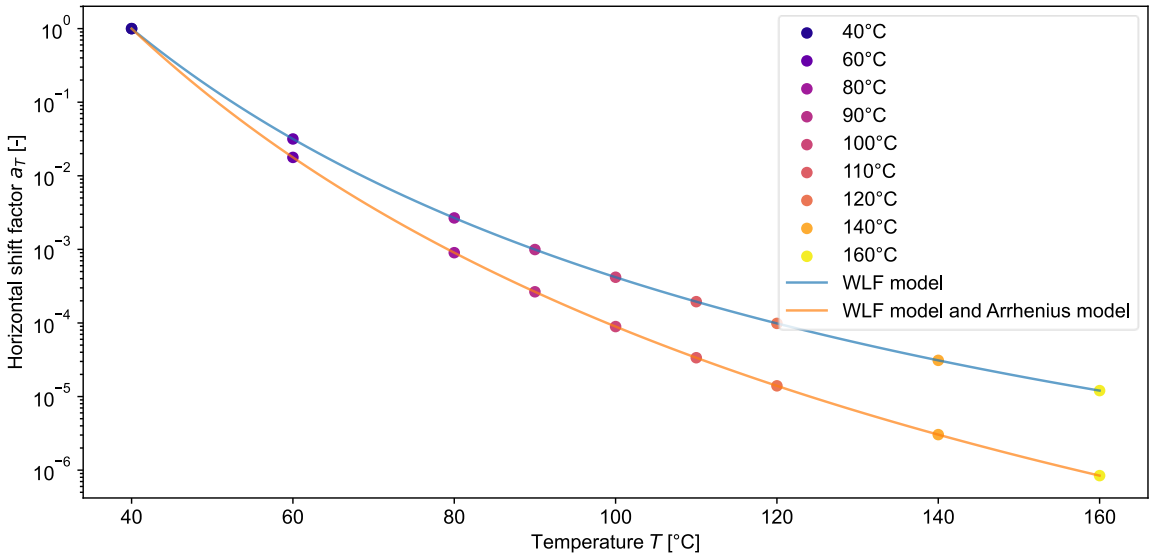

Figure 4.6.8: Comparison of the horizontal shift factors for the sample PEHMA-v (90,000 g/mol) (α = 10%) using the Williams-Landel-Ferry model with $C_1 = 9.0435$ and $C_2 = 100.61$ (blue curve), and with the addition of the Arrhenius model (orange curve) where the activation energy for flow is set to $E_a = 25{,}000$ J/mol.

One observes that the Arrhenius equation provides a supplementary correction that increases in magnitude as the temperature rises. This larger temperature dependence on the viscoelastic properties observed for the vitrimer is in line with the properties usually observed for supramolecular and reversible networks.

4.6.3 PEHMA-v (90,000 g/mol) (α = 20%)

The material PEHMA-v (90,000 g/mol) (α = 20%) is characterized using Small Amplitude Oscillatory Shear (SAOS). As for the previous sample, it contains dynamic covalent bonds in its structure but in greater number. The experiments are performed at several temperatures to build a master curve. The experimental data for this sample is illustrated in Figure 4.6.9.

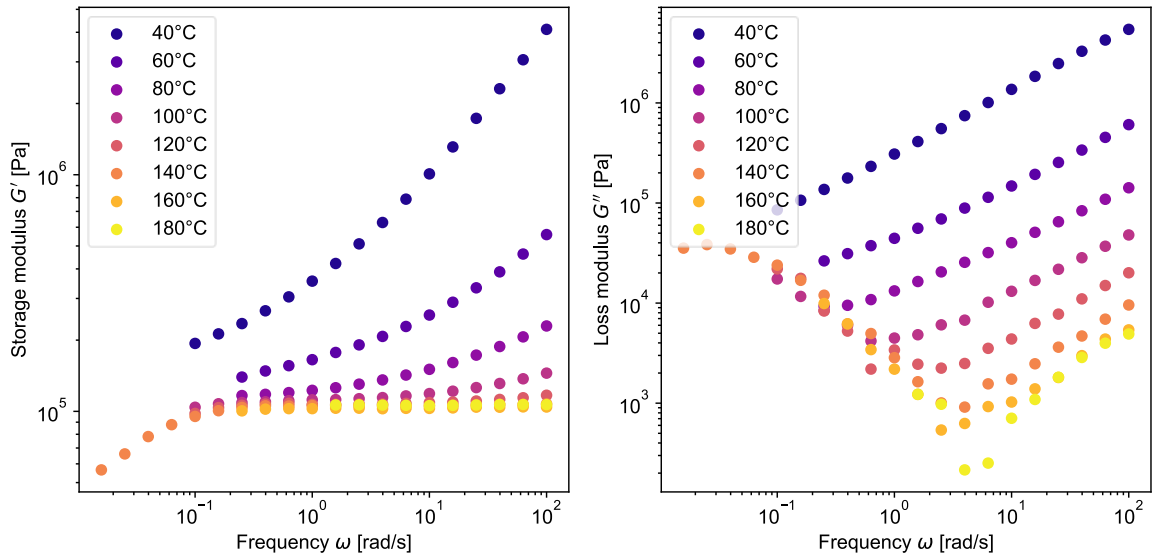

Figure 4.6.9: Experimental data for the storage and loss moduli of the sample PEHMA-v (90,000 g/mol) (α = 20%) from Small Amplitude Oscillatory Shear (SAOS) performed at 40°C, 60°C, 80°C, 90°C, 100°C, 110°C, 120°C, 140°C and 160°C.

A master curve can be constructed using the Time Temperature Superposition principle. The reference temperature is set to 40°C, as for the previous samples. The Williams-Landel-Ferry model is applied to the experimental curves with the same values, $C_1 = 9.0435$ and $C_2 = 100.61$. The vertical shifts are also set to 1 as the chemistry is considered to not change. The master curves are shown in Figure 4.6.10.

A good superposition is observed in the low frequency range (below 10^{-3} rad/s) at which a rubbery plateau is observed, and in the high frequency range, above 10^{0} rad/s, for the storage modulus. However, it is important to note that the curves do not superpose in the intermediate range, between 10^{-3} rad/s and 10^{0} rad/s. One may assume that the Arrhenius model could resolve this issue by accounting for the activation energy for flow. Interestingly, the best superposition occurs when the activation energy for flow is set to 0 J/mol or to negative values.

Indeed, looking at the loss modulus data shifted with WLF equation, it seems that the higher the temperature is, the longer the sample will take to relax. Due to this unexpected behaviour, which is further discussed with the PS vitrimers, the Arrhenius model could not be applied to the data. This requires further investigation, as such temperature dependence has never been reported in literature. A similar behaviour has been recently observed for a similar vitrimer (but with a different backbone chemistry) in the group of Professor Renaud Nicolaÿ at ESPCI, which seems to indicate that this property applies to this type of samples i.e., entangled vitrimers based on ester-boronic crosslinks.

NOTE

One might be intrigued by the curve corresponding to 180°C in Figure 4.6.10, because of the small number of experimental points. This measurement was conducted last to confirm the value of the plateau at 10^5 Pa.

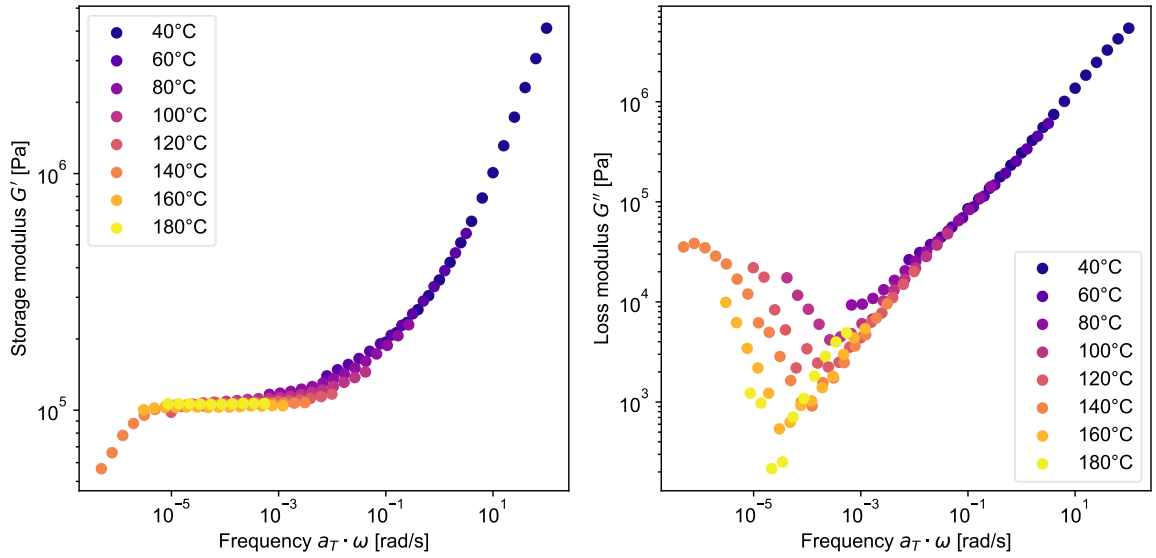

Figure 4.6.10: Master curve of the storage and loss moduli of the sample PEHMA-v (90,000 g/mol) (α = 20%) using the Williams-Landel-Ferry model with $C_1 = 9.0435$ and $C_2 = 100.61$.

It seems important to compare the experimental curves, specifically the storage moduli, of the different samples being studied. This comparison can provide a more comprehensive understanding of the impact of incorporating vitrimers. Figure 4.6.11 presents the storage moduli of the investigated samples at temperatures of 40°C, 60°C, 100°C and 160°C.

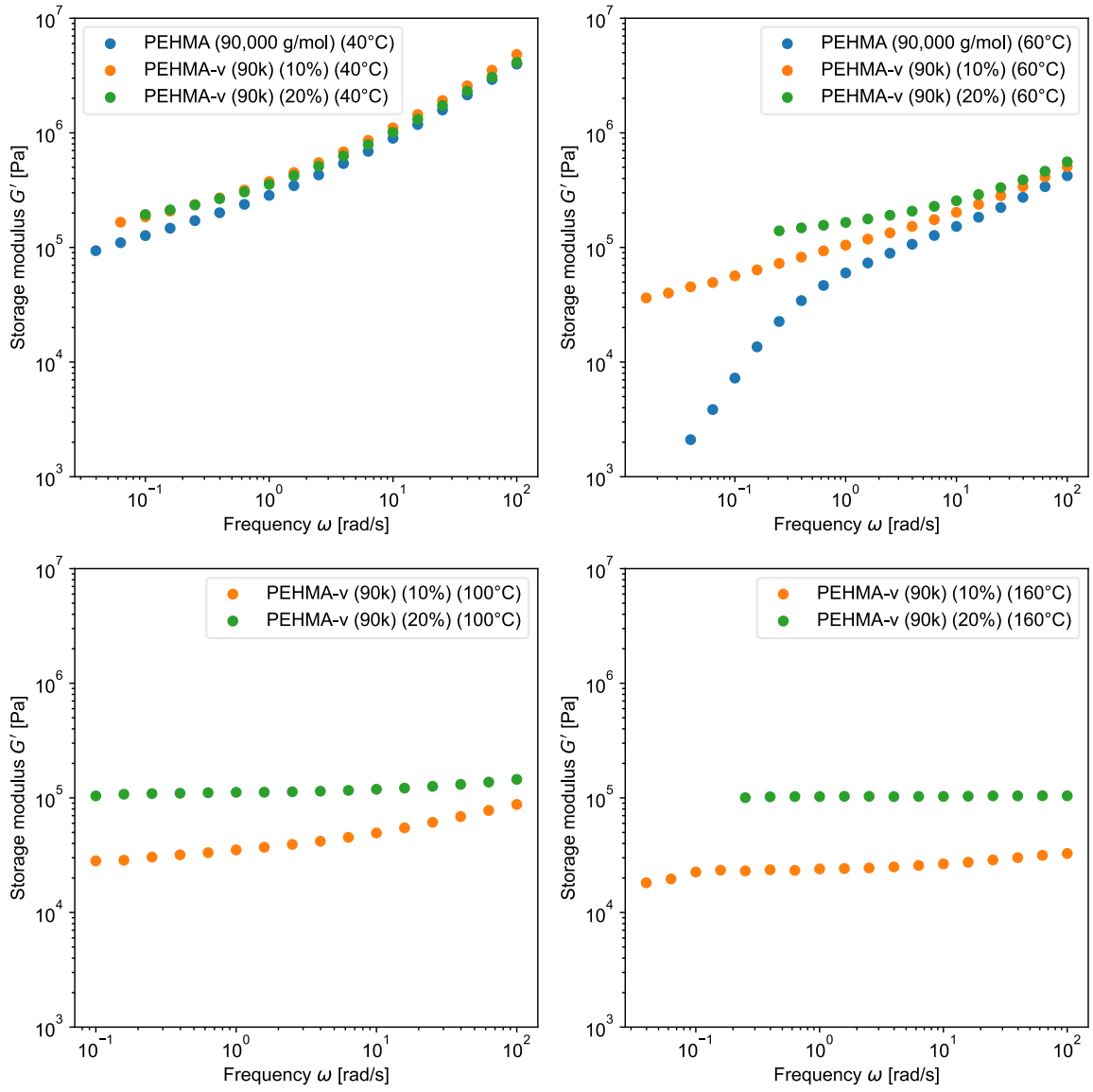

Figure 4.6.11: Comparison of the experimental storage moduli of PEHMA (90,000 g/mol), PEHMA-v (90,000 g/mol) (α = 10%) and PEHMA-v (90,000 g/mol) (α = 20%). The curves of the storage modulus for PEHMA (90,000 g/mol) could not be determined at 100°C and 160°C as the material flows at these temperatures.

At low temperatures (40°C and 60°C), the curve overlap in the high frequency range corresponds to the Rouse regime, which refers to the local motions of the chains, and is not affected by the presence of covalent dynamic bonds. Upon observation at high temperatures, a new plateau emerges at $2 \cdot 10^4$ Pa for PEHMA-v (90,000 g/mol) (α = 10%) and 10^5 Pa for PEHMA-v (90,000 g/mol) (α = 20%), indicating the presence of a crosslinking network, which prevents the Rouse relaxation of sub-chains longer than the length of the sub-chains located between

two cross-linking points. This cross-linking between the polymer chains improves the mechanical properties of the material. Furthermore, both vitrimer samples start to flow at a temperature of 160°C (see Figures 4.6.5 and 4.6.9), which confirms vitrimer materials are capable of being processed and reshaped.

Section 4.7 Viscoelastic Properties of PS-based samples

This section describes the rheological experiments performed on the PS-based samples. As for PEHMA-based samples, it is observed that the addition of vitrimers improves the mechanical properties compared to the base material. A new plateau appears in the storage modulus and its value also increases with the number of dynamic covalent bonds present in the material. The materials are also able to flow at high temperature, enabling their processing. The activation energy for flow is estimated via the Arrhenius model.

4.7.1 PS-p (50,000 g/mol)

As a first step, the vitrimer precursor PS-p (50,000 g/mol) is characterized using Small Amplitude Oscillatory Shear (SAOS). This sample serves as a baseline for understanding the influence of the addition of dynamic covalent bonds to the material. It is important to remind that PEHMA-based samples and PS-based samples have the same degree of polymerization (DP = 450). The experiments are performed at several temperatures in order to build a master curve. The experimental data for the PS-p (50,000 g/mol) sample is illustrated in Figure 4.7.1.

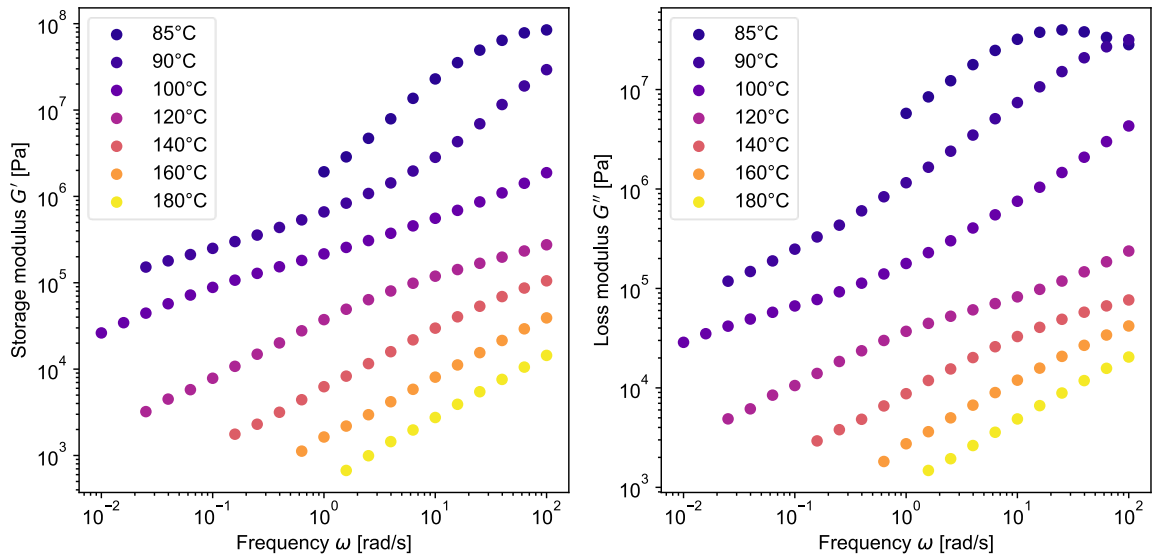

Figure 4.7.1: Experimental data for the storage and loss moduli of the sample PS-p (50,000 g/mol) from Small Amplitude Oscillatory Shear (SAOS) performed at 85°C, 90°C, 100°C, 120°C, 140°C, 160°C, and 180°C.

A master curve can be constructed using the Time Temperature Superposition principle. As seen in Section 4.4, to apply the Williams-Landel-Ferry model, it is important to know the precise values of the constants C_1 and C_2 to shift the experimental data sets. However, these values are not readily available in literature and the values found for the pure PS cannot be used anymore. Indeed, using $C_1 = 8.40$ and $C_2 = 80.0$ found in Section 4.4 results in a poor superposition of the curves. Adding a comonomer largely influences the flexibility of the chain and a change in the glass transition temperature is noted compared to PS (Total Energies): while the PS sample has a glass transition temperature of 106.6°C, the one for the precursor has been evaluated to 65.2°C. The ARES software TA Orchestrator is therefore used to determine the optimal shift factors in order to create a master curve for the investigated sample. The Williams-Landel-Ferry model is then fitted with these parameters to determine the values of C_1 and C_2. The horizontal and vertical shift factors are shown in Figure 4.7.2.

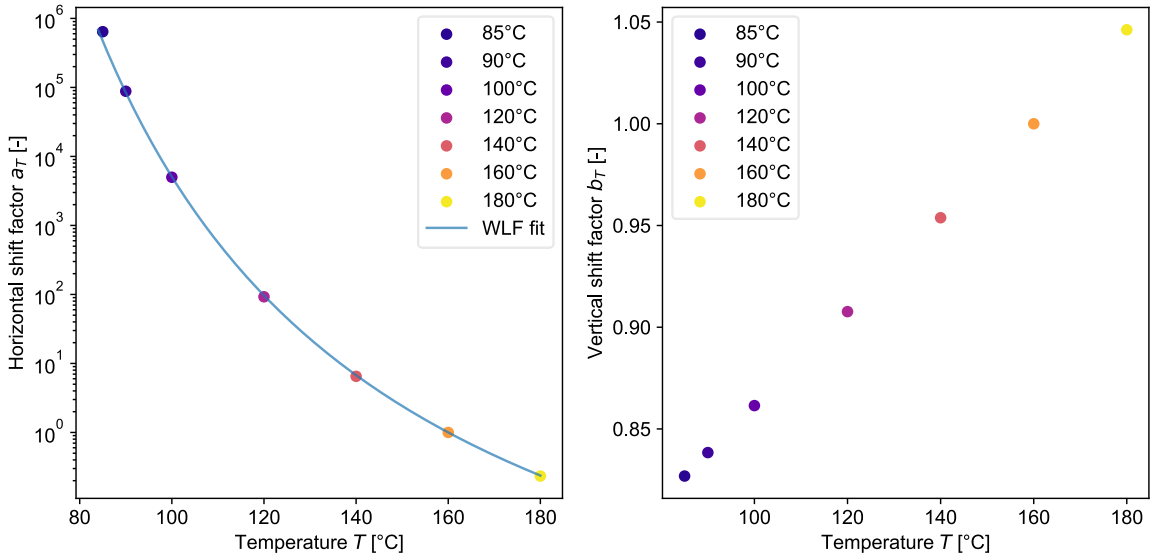

Figure 4.7.2: Horizontal and vertical shift factors for the PS-p (50,000 g/mol) determined using the ARES software at a reference temperature of 160°C. A Williams-Landel-Ferry (WLF) curve fit is performed on the horizontal shift factors.

The values of the constants in the Williams-Landel-Ferry model are determined as $C_1 = 5.0534$ and $C_2 = 141.8$ and a very good fit is observed. These values allow the construction of the master curves of the storage and loss moduli for the investigated sample, as shown in Figure 4.7.3.

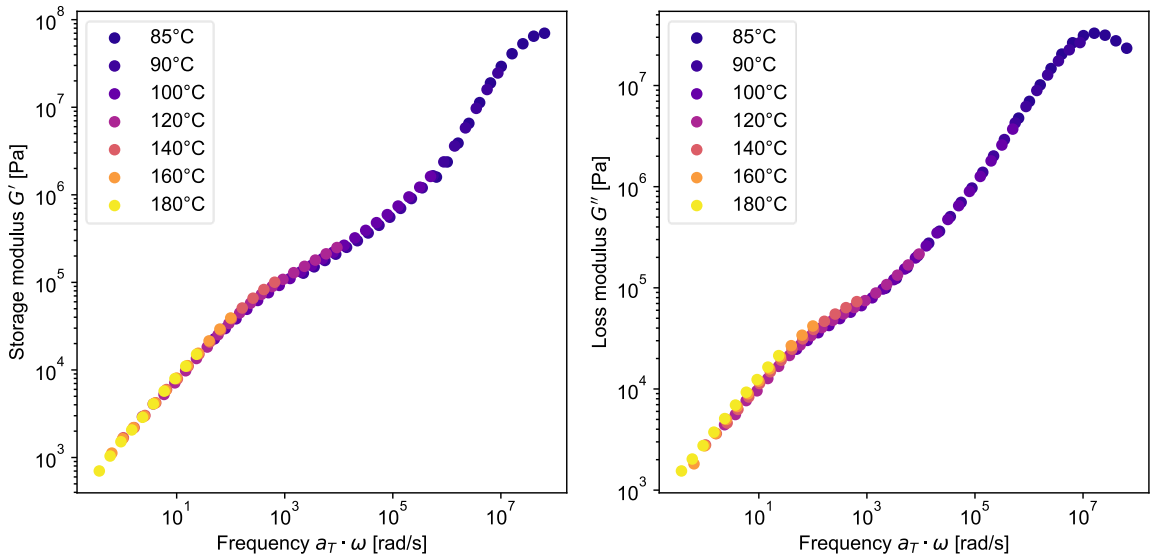

Figure 4.7.3: Master curves of the storage and loss moduli for the sample PS-p (50,000 g/mol) at a reference temperature of 160°C using the Williams-Landel-Ferry model with $C_1 = 5.0534$ and $C_2 = 141.8$.

4.7.2 PS-v (50,000 g/mol) (α = 10%)

Dynamic covalent bonds are then inserted into the previous sample i.e., PS-p (50,000 g/mol), to obtain the vitrimer material PS-v (50,000 g/mol) (α = 10%). This sample is characterized by a 10% crosslinking ratio noted by α = 10%. The experimental data for the measured storage and loss moduli of this sample is illustrated in Figure 4.7.4.

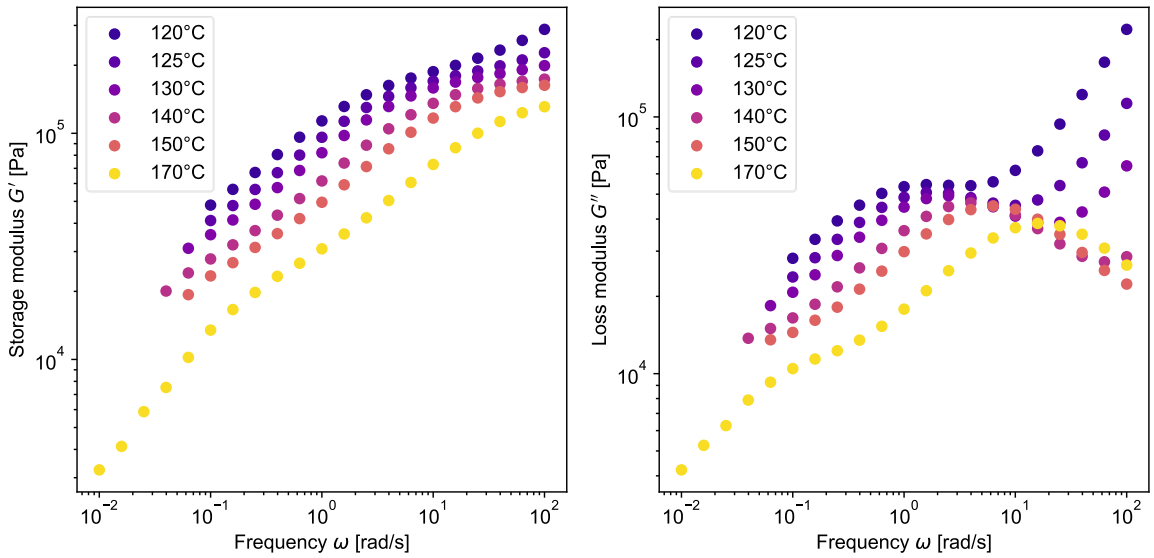

Figure 4.7.4: Experimental data for the storage and loss moduli of the sample PS-v (50,000 g/mol) (α = 10%) from Small Amplitude Oscillatory Shear (SAOS) performed at 120°C, 125°C, 130°C, 140°C, 150°C, and 170°C.

A master curve can be constructed using the Time Temperature Superposition principle. The Williams-Landel-Ferry model is applied to the experimental curves. The values used for the horizontal shift factors are $C_1 = 5.0534$ and $C_2 = 141.8$, found for the previous sample, because the materials share the same molecular chemistry. All vertical shift factors are set to 1. This is an acceptable approximation as Figure 4.7.2 shows that the vertical shift factors range between 0.85 and 1.05. The master curves of the storage and loss moduli are shown in Figure 4.7.5.

Observations reveal that, as expected, a good superposition of the data is observed in the storage modulus at high frequencies, specifically above 10^3 rad/s. Then, it is clear that the experimental data does not superpose in the intermediate regime i.e., between 10^{-2} rad/s and 10^3 rad/s. This is attributed to the different temperature dependence of the bond exchange

dynamics. However, as for the PEHMA-v (90,000 g/mol) (α = 20%), the influence of temperature is found to be the inverse of the expected one: the higher the temperature, the slower is this intermediate relaxation. Accounting for such an effect with the Arrhenius equation would therefore require imposing a negative activation energy.

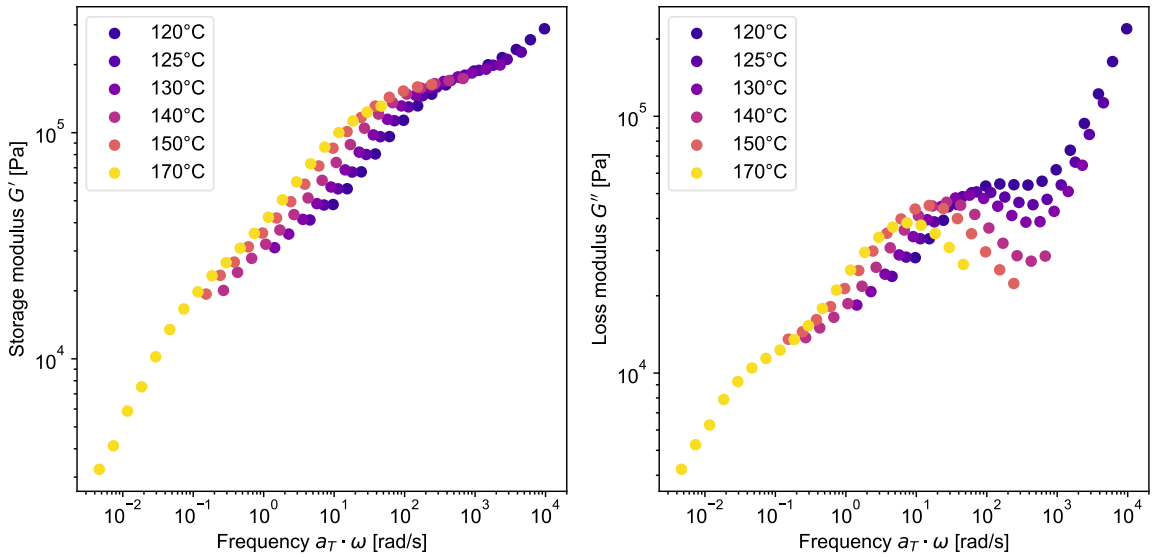

Figure 4.7.5: Master curves of the storage and loss moduli for the sample PS-v (50,000 g/mol) (α = 10%) at a reference temperature of 160°C using the Williams-Landel-Ferry model with $C_1 = 5.0534$ and $C_2 = 141.8$.

Looking at the unshifted data (see Figure 4.7.4), one sees, however, that an increase of the temperature speeds up the intermediate relaxation i.e., showing the usual trend for a polymeric sample. Therefore, the counterintuitive result presented in Figure 4.7.5 seems to come from the large temperature dependence of the high frequency region, which is unexpectedly larger than the temperature dependence found in the intermediate region. Consequently, when the master curve is built in the high frequency region by applying the Williams-Landel-Ferry equation, the shift factors to be applied in the intermediate region have a negative activation energy for flow.

In order to further investigate this effect, the raw data are horizontally shifted manually to ensure a good superposition of the storage modulus in the intermediate region, and the corresponding shift factors are plotted on Figure 4.7.6. It is observed that the latter follow an Arrhenius dependence, with an activation energy for flow of approximately $E_a = 100{,}000$ J/mol. The corresponding master curves are plotted in Figure 4.7.7.

The observations made are quite intriguing, as they suggest that the equation utilized for calculating the horizontal shift factors may not be applicable to this particular type of vitrimer. Rather than multiplying the William-Landel-Ferry component (equation 2.2.2) with the Arrhenius component (equation 2.2.3), these two components are decoupled. This discovery has significant implications for the field and warrants further investigation, as it contradicts the behaviour observed with supramolecular polymers and the model proposed by Colby and coworkers.

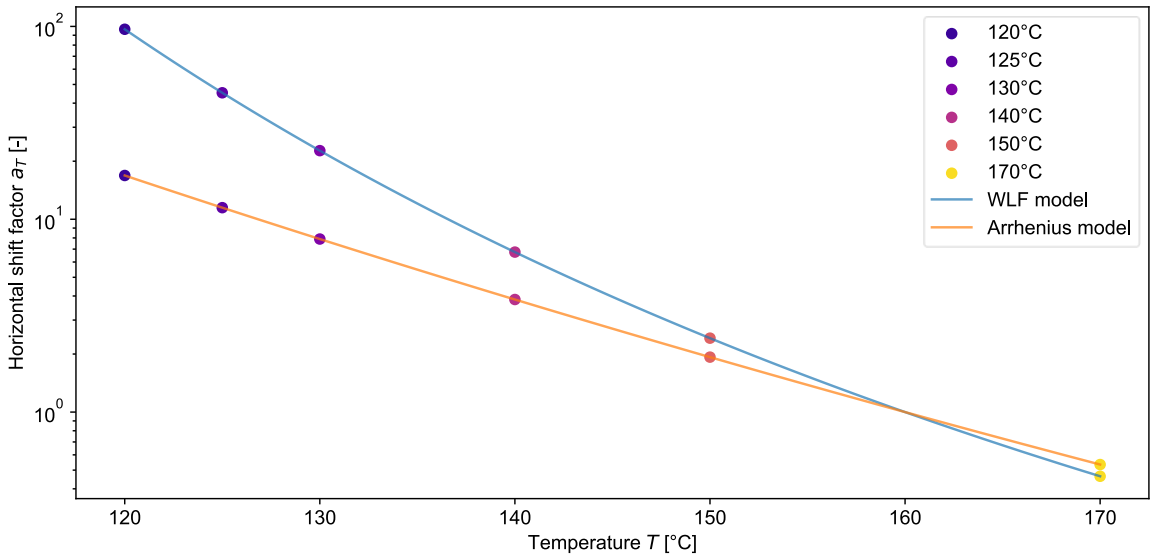

Figure 4.7.6: Comparison of the horizontal shift factors for the sample PS-v (50,000 g/mol) (α = 10%) using the Williams-Landel-Ferry model with $C_1 = 5.0534$ and $C_2 = 141.8$ (blue curve), and the Arrhenius model (orange curve) where the activation energy for flow is set to $E_a = 25{,}000$ J/mol.

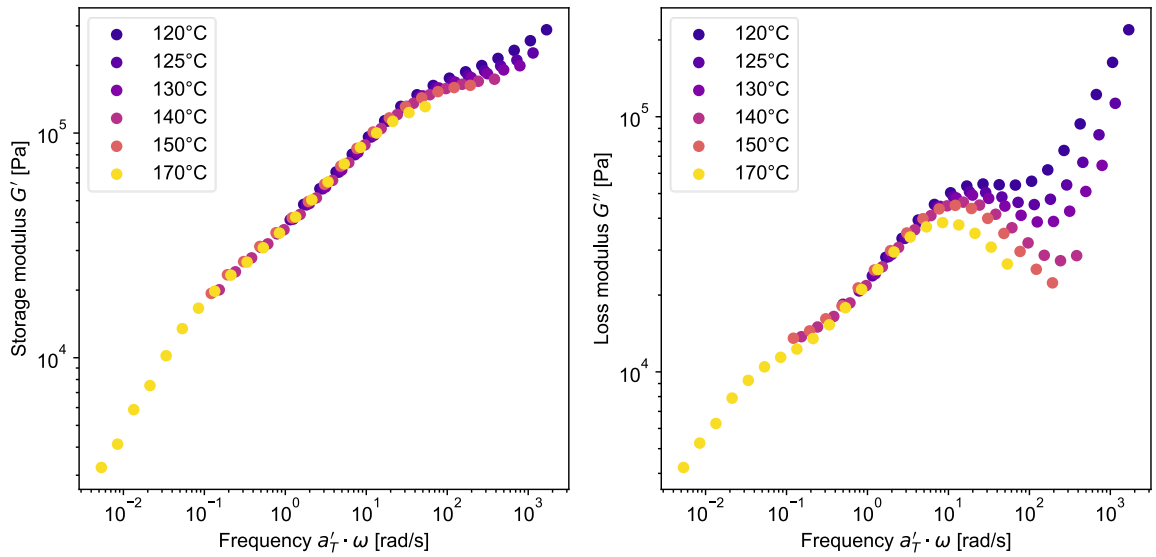

Figure 4.7.7: Master curves of the storage and loss moduli for the sample PS-v (50,000 g/mol) (α = 10%) at a reference temperature of 160°C using the Arrhenius model with E = 100,000 J/mol.

4.7.3 PS-v (50,000 g/mol) (α = 20%)

As for the previous material, this sample presents dynamic covalent bonds. Its specificity is however that the crosslinking ration is two times more, reaching α = 20%. The experimental data for the measured storage and loss moduli of this sample is illustrated in Figure 4.7.8.

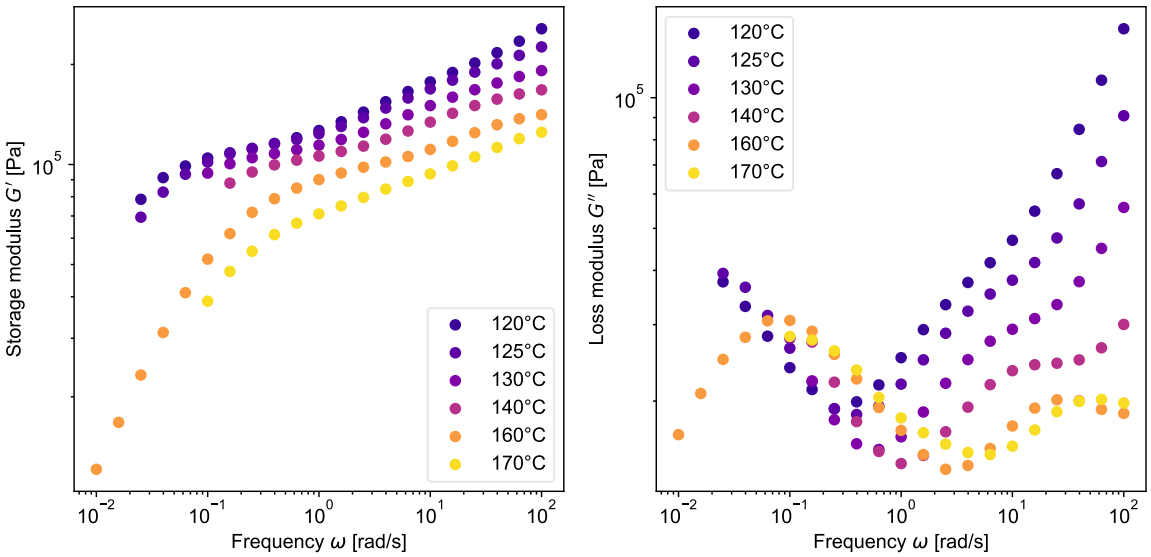

Figure 4.7.8: Experimental data for the storage and loss moduli of the sample PS-v (50,000 g/mol) (α = 20%) from Small Amplitude Oscillatory Shear (SAOS) performed at 120°C, 125°C, 130°C, 140°C, 160°C and 170°C.

Again, a master curve can be constructed using the Time Temperature Superposition principle. The refence temperature is set at 40°C, as for the previous samples. The Williams-Landel-Ferry model is applied to the experimental curves with the same values, $C_1 = 5.0534$ and $C_2 = 141.8$. The vertical shift factors are also set to 1 as the chemistry is considered to not change. The master curves are shown in Figure 4.7.9.

An observable superposition is identified at high frequency, but it appears to be flawed in the intermediate frequency range of 10^{-1} rad/s to 10^{3} rad/s. One may assume that the Arrhenius model could resolve this issue by accounting for the activation energy for flow. However, as for PEHMA-v (90,000 g/mol) (α = 20%), the best superposition occurs when the activation energy for flow is set to 0 J/mol. This suggests that there is yet again another relaxation process that must be considered, and further investigation is required to fully comprehend this phenomenon.

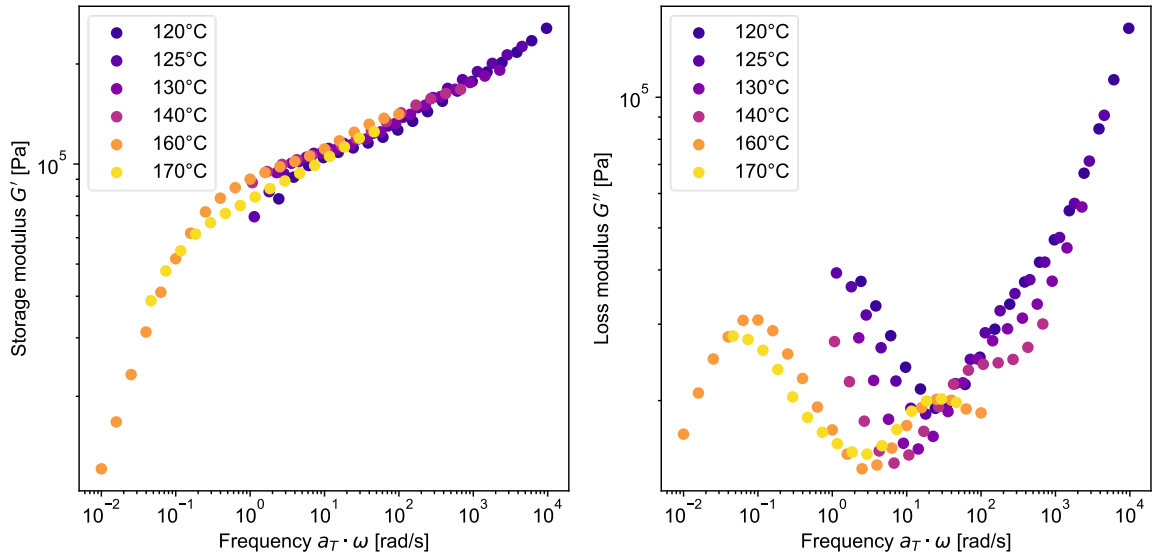

Figure 4.7.9: Master curves of the storage and loss moduli for the sample PS-v (50,000 g/mol) (α = 20%) at a reference temperature of 160°C using the Williams-Landel-Ferry model with C1 = 5.0534 and C2 = 141.8.

As for PEHMA-based samples, it seems important to compare experimental curves, specifically the storage moduli, of the of the PS-based samples under investigation. This comparison can provide a more comprehensive understanding of the impact of incorporating vitrimers. Figure 4.7.10 presents the storage moduli of the investigated samples at temperatures of 120°C and 170°C (160°C for PS-p (50,000 g/mol) as no measurement was performed at temperature 170°C).

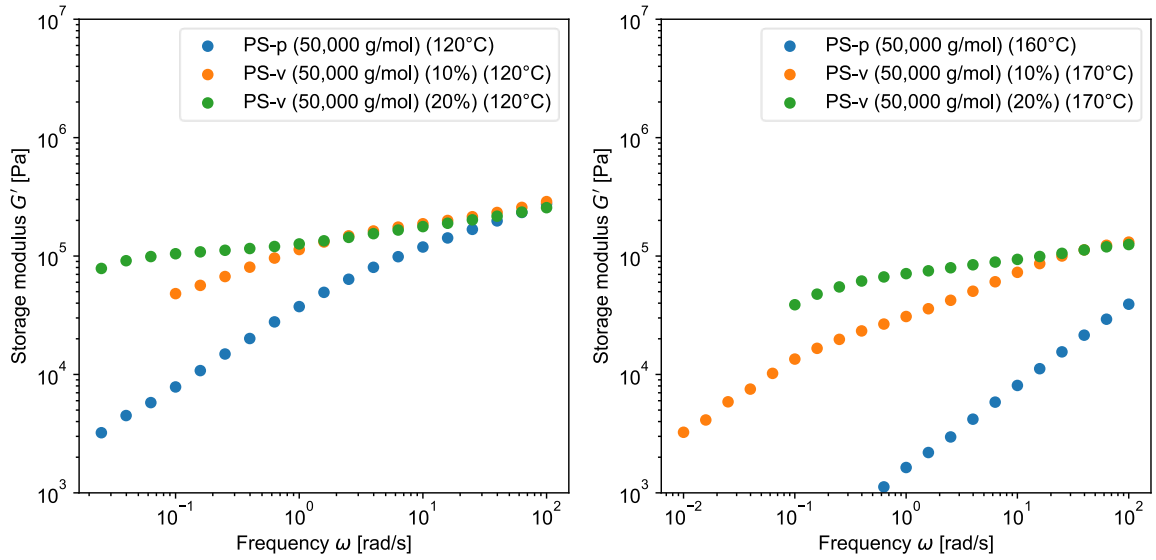

Figure 4.7.10: Comparison of the experimental storage moduli of PS-p (50,000 g/mol), PS-v (50,000 g/mol) (α = 10%) and PS-v (50,000 g/mol) (α = 20%) at 120°C and 170°C (160°C for PS-p (50,000 g/mol)).

Upon observation at high temperatures, it appears that the plateau at 10^5 Pa is extended for both vitrimer materials. Also, a new plateau emerges at 10^4 Pa for PS-v (50,000 g/mol) (α = 10%) which indicates the formation of a crosslinking network. This would suggest that the prolonged plateau visible for PS-v (50,000 g/mol) (α = 20%) is actually composed of two plateaus, namely the entanglement plateau (at high frequency) and the crosslinking plateau (at lower frequency), which have nearly the same level. This crosslinking between the polymer chains improves the mechanical properties of the material. Furthermore, both vitrimer samples exhibit flow behaviour, which confirms vitrimer materials are capable of being processed and reshaped.

Part 5 Conclusion and Perspectives

The data published in 2022 by the Organization for Economic Cooperation and Development (OECD) showed that only 10% of plastic waste is recycled. However, the European Union aims at reaching 50% by 2030. Achieving this goal implies solving the incompatibility issues related to contaminated waste. Compatibilization solutions currently exist for specific polymers, but it is hoped that vitrimers may offer a universal approach.

The purpose of this research project is to understand the influence of adding low concentrations of vitrimers to a well-defined immiscible polymer blend, in order to reinforce the polymer-polymer interface allowing to obtain recycled polymers with enhanced mechanical properties.

A particular attention was paid in selecting the two main polymers for this study: poly(styrene) (PS) and poly(2-ethyl hexyl methacrylate) (PEHMA). Their properties were measured with different analytical techniques (Differential Scanning Calorimetry (DSC) and Gel Permeation Chromatography (GPC)). Atomic Force Microscopy (AFM) performed on their blends confirmed the phase separation, regardless of the sample preparation method.

Rheometry being identified as the technique that effectively connects the molecular structures of the polymers with their macroscopic mechanical properties, the viscoelastic properties of PS and PEHMA polymers were measured using Small Amplitude Oscillatory Shear (SAOS) experiments, and master curves have been successfully constructed using the Williams-Landel-Ferry (WLF) model.

Avoiding the degradation of the PS and PEHMA polymers during the preparation and measurement was the main encountered challenge with these samples. Several preparation methods were tested, and the method qualification was performed by comparing the rheological curves with the data provided in the literature for poly(styrene). The obtained experimental master curves allowed to validate the program implementing the Time Marching Algorithm

with established parameters. For reliable results with AFM, blend preparation methods have been designed to ensure that the sample surface is plane and smooth.

The rheological experiments have been further applied on vitrimer materials based on PS and PEHMA and the obtained results demonstrate the successful formation of a chemical network. For PS and modified PS, the SAOS curves measured between 10^{-1} rad/s and 10^{2} rad/s at different temperatures can be shifted into a master curve using the WLF model. However, when adding the cross-linkers to form a chemical network, the WLF model is not successful in creating a master curve: the curves do not overlay in an intermediate range of frequencies. Such temperature dependence, which is thought to be related to the presence of the dynamic bonds, has never been reported in literature. Repeated experiments provided similar results proving that the phenomenon is real. This has also been observed on PEHMA vitrimers, as well as confirmed by other laboratories. Furthermore, both PS and PEHMA based vitrimers showed enhanced mechanical properties and retained their ability to flow at high temperature, thus demonstrating the dynamic nature of the covalent bonds.

This first study allows to further investigate the changes at the interface of the blends of PS based vitrimer and PEHMA based vitrimer as well as to understand how the dynamics of the vitrimers depends on several parameters such as the temperature, the nature of the vitrimers, or the density of cross-linkers. The final goal is to demonstrate the possibility to obtain better mechanical properties by adding a small quantity of vitrimer in a blend of incompatible thermoplastics. This project will be continued in the following months, through a PhD program.

References

[1] D. Dadachanji, "Uses of Thermoplastics," Sciencing, [Online] Available at: https://sciencing.com/uses-thermoplastics-2457.html (accessed May 26, 2023)

[2] Ansys GRANTA EduPack software (2022 edition) Cambridge, United Kingdom [Online] Available at: www.ansys.com/materials (accessed May 26, 2023)

[3] M. Revels, "New method for thermoplastic production offers potential to replace metals," Texas A&M University Engineering, [Online] Available at: https://engineering.tamu.edu/news/2022/04/etid-new-method-for-thermoplastic-production-offers-potential-to-replace-metals.html (accessed May 26, 2023)

[4] Thomas Corporation, "Comparison of Thermoset Versus Thermoplastic Materials," [Online] Available at: https://www.thomasnet.com/articles/plastics-rubber/thermoset-vs-thermoplastics/ (accessed May 26, 2023)

[5] J.-M. Lehn, "Dynamers: dynamic molecular and supramolecular polymers," *Progress in Polymer Science,* vol. 30, no. 8-9, pp. 814-831, 2005, doi: 10.1016/j.progpolymsci.2005.06.002

[6] C. J. Kloxin, T. F. Scott, B. J. Adzima, and C. N. Bowman, "Covalent Adaptable Networks (CANs): A Unique Paradigm in Crosslinked Polymers," *Macromolecules,* vol. 43, no. 6, pp. 2643-2653, Mar 23 2010, doi: 10.1021/ma902596s.

[7] D. Montarnal, M. Capelot, F. Tournilhac, and L. Leibler, "Silica-like malleable materials from permanent organic networks," *Science,* vol. 334, no. 6058, pp. 965-8, November 18 2011, doi: 10.1126/science.1212648.

[8] M. Röttger, T. Domenech, R. van der Weegen, A. Breuillac, R. Nicolaÿ, and L. Leibler, "High-performance vitrimers from commodity thermoplastics through dioxaborolane metathesis," *Science,* vol. 356, no. 6333, American Association for the Advancement of Science (AAAS), pp. 62-65, April 7 2017, doi: 10.1126/science.aah5281.

[9] N. J. Van Zee and R. Nicolaÿ, "Vitrimer Chemistry and Applications," in *Macromolecular Engineering*, 2022, pp. 1-38.

[10] M. Hayashi, "Implantation of Recyclability and Healability into Cross-Linked Commercial Polymers by Applying the Vitrimer Concept," *Polymers (Basel),* vol. 12, no. 6, Jun 10 2020, doi: 10.3390/polym12061322.

[11] R. Geyer, J. R. Jambeck, and K. L. Law, "Production, use, and fate of all plastics ever made," *Sci Adv,* vol. 3, no. 7, p. e1700782, July 19 2017, doi: 10.1126/sciadv.1700782.

[12] OECD. Plastics use in 2019 [Online] Available at: https://www.oecd-ilibrary.org/content/data/efff24eb-en

[13] OECD. Plastics use by region - projections [Online] Available at: https://www.oecd-ilibrary.org/content/data/913b14f3-en

[14] European Parliament. "Plastic waste and recycling in the EU: facts and figures: News: European Parliament." European Parliament. [Online] Available at: https://www.europarl.europa.eu/news/en/headlines/society/20181212STO21610/plastic-waste-and-recycling-in-the-eu-facts-and-figures (accessed April 15, 2023)

[15] OECD. Plastic waste by end-of-life fate and region - projections [Online] Available at: https://www.oecd-ilibrary.org/content/data/e4e8c086-en

[16] (2018). Communication from the Commission to the European Parliament , the Council, the European Economic and Social Committee and the Committee of the Regions - *A European Strategy for Plastics in a Circular Economy*

[17] European Council, "European Green Deal – Consilium," Europa, [Online] Available at: https://www.consilium.europa.eu/en/policies/green-deal/ (accessed April 15, 2023).

[18] J. M. Dealy, D. J. Read, and R. G. Larson, *Structure and Rheology of Molten Polymers: From Structure to Flow Behavior and Back Again*. Carl Hanser Verlag GmbH & Company KG, 2018.

[19] F. R. Schwarzl, "The numerical calculation of storage and loss compliance from creep data for linear viscoelastic materials," *Rheologica Acta,* vol. 8, no. 1, pp. 6-17, 1969/03/01 1969, doi: 10.1007/BF02321350.

[20] F. R. Schwarzl, "Numerical calculation of storage and loss modulus from stress relaxation data for linear viscoelastic materials," *Rheologica Acta,* vol. 10, no. 2, pp. 165-173, 1971/06/01 1971, doi: 10.1007/BF02040437.

[21] F. R. Schwarzl, "Numerical calculation of stress relaxation modulus from dynamic data for linear viscoelastic materials," *Rheologica Acta,* vol. 14, no. 7, pp. 581-590, 1975/07/01 1975, doi: 10.1007/BF01520809.

[22] D. J. Plazek, "1995 Bingham Medal Address: Oh, thermorheological simplicity, wherefore art thou?," *Journal of Rheology,* vol. 40, no. 6, pp. 987-1014, 1996, doi: 10.1122/1.550776.

[23] P. E. Rouse, "A Theory of the Linear Viscoelastic Properties of Dilute Solutions of Coiling Polymers," *The Journal of Chemical Physics,* vol. 21, no. 7, pp. 1272-1280, 1953, doi: 10.1063/1.1699180.

[24] E. Ruymbeke and D. Vlassopoulos, "Macromolecular Rheology," in *Macromolecular Engineering*, 2022, pp. 1-56.

[25] P. de Gennes, *Scaling concepts in polymer physics*. Ithaca u.a.: Cornell Univ. Pr., 1979.

[26] M. Doi and S. F. Edwards, *The Theory of Polymer Dynamics*. Clarendon Press, 1988.

[27] E. van Ruymbeke, C. Bailly, R. Keunings, and D. Vlassopoulos, "A General Methodology to Predict the Linear Rheology of Branched Polymers," *Macromolecules,* vol. 39, no. 18, pp. 6248-6259, 2006, doi: 10.1021/ma0604385.

[28] M. Bousmina and N. Mechbal, "Experimental study of interfacial slip effect on the rheological behavior of PS/PMMA blends," 2011, doi: 10.34874/IMIST.PRSM/FSEJOURNAL-V1I1.26937.

[29] L. A. Utracki and C. A. Wilkie, *Polymer Blends Handbook*. Dordrecht: Springer Netherlands, 2014.

[30] V. Mironov, *Fundamentals of Scanning Probe Microscopy*. Nizhniy Novgorod, Russia: The Russian Academy of Sciences, Institute of Physics of Microstructures, 2004, p. 98.

[31] N. Somanathan, A. Sanjay, and V. Arumugam, "Compatibility studies on polystyrene and poly-n-butyl methacrylate," *Journal of Applied Polymer Science,* vol. 83, no. 11, pp. 2322-2330, 2002, doi: 10.1002/app.10111.

[32] Sigma Aldrich (Belgium) Thermal Transitions of Homopolymers: Glass Transition and Melting Point [Online] Available at: https://www.sigmaaldrich.com/BE/en/technical-documents/technical-article/materials-science-and-engineering/polymer-synthesis/thermal-transitions-of-homopolymers

[33] Crow. Polymer Database Glass Transition Temperatures [Online] Available at: https://polymerdatabase.com/polymer%20physics/Polymer%20Tg%20C.html

[34] J. C. Moore, "Gel permeation chromatography – A new method for molecular weight distribution of high polymers," *Journal of Polymer Science Part A: General Papers,* vol. 2, no. 2, pp. 835-843, 1964, doi: 10.1002/pol.1964.100020220.

[35] A. Jonas, UCLouvain - Ecole Polytechnique de Louvain (EPL), *LMAPR2261 - Polymer Chemistry and Physical Chemistry (Notes de cours)*. Louvain-la-Neuve, Belgium: Service d'Impression du Cercle Industriel (SICI), 2021, p. 9.

[36] A. Kovalenko, T. Brunet, and O. Mondain-Monval, "Mechanical and acoustic properties of macroporous acrylate materials near glass transition," *Polymer,* vol. 148, pp. 239-246, 2018, doi: 10.1016/j.polymer.2018.06.033.

[37] H. Watanabe, T. Sakamoto, and T. Kotaka, "Entanglements in linear polystyrenes," *Macromolecules,* vol. 18, no. 7, pp. 1436-1442, 2002, doi: 10.1021/ma00149a014.

[38] H. Lentzakis *et al.*, "Constraint Release Mechanisms for H-Polymers Moving in Linear Matrices of Varying Molar Masses," *Macromolecules,* vol. 52, no. 8, pp. 3010-3028, 2019, doi: 10.1021/acs.macromol.9b00251.

[39] C. Hannecart, C. Clasen, and E. van Ruymbeke, "Constraint Release Rouse Mechanisms in Bidisperse Linear Polymers: Investigation of the Release Time of a Short-Long Entanglement," *Polymers (Basel),* vol. 15, no. 6, Mar 21 2023, doi: 10.3390/polym15061569.

UNIVERSITÉ CATHOLIQUE DE LOUVAIN
École polytechnique de Louvain
Rue Archimède, 1 bte L6.11.01, 1348 Louvain-la-Neuve, Belgique | **www.uclouvain.be/epl**